Expressing human Orai3 in insect cells for pharmacological studies

A thesis submitted in partial fulfillment
of the requirements for the degree of
Master of Science

by

Orville R. Bennett
B.S., University of Hartford, 2005

2012
Wright State University

Wright State University
GRADUATE SCHOOL

January 17, 2012

I HEREBY RECOMMEND THAT THE THESIS PREPARED UNDER MY SUPERVISION BY Orville R. Bennett ENTITLED Expressing human Orai3 in insect cells for pharmacological studies BE ACCEPTED IN PARTIAL FULFILLMENT OF THE REQUIREMENTS FOR THE DEGREE OF Master of Science.

J. Ashot Kozak, Ph. D.
Thesis Director

Timothy Cope, Ph. D.
Chair, Department of Neuroscience,
Cell Biology and Physiology

Committee on
Final Examination

J. Ashot Kozak, Ph. D.

Thomas Brown, Ph. D.

Adrian Corbett, Ph. D.

Robert Putnam, Ph. D.

Andrew Hsu, Ph.D.
Dean, Graduate School

ABSTRACT

Bennett, Orville. M.S., Department of Neuroscience, Cell Biology and Physiology, Wright State University, 2012. *Expressing human Orai3 in insect cells for pharmacological studies.*

The Orai3 protein forms a Ca^{2+} channel with a pharmacological profile distinct from its close relative, the store-operated Ca^{2+} channel Orai1. Though closely related to Orai1, the function of Orai3 in humans is still unclear. This study attempts to contribute to the body of knowledge by undertaking a pharmacological analysis of Orai3 in insect cells. We describe here the creation of a vector capable of expressing the mammalian Orai3 gene on an insect background. We demonstrate the ability to induce gene expression of Orai3 in these insect cells, and then assess the effectiveness of this system by characterizing the pharmacological properties with the drug 2-aminoethoxydiphenyl borate (2-APB). The results show that the current strategy used to express Orai3 will require additional refinement before the system can be considered generally useful for pharmacological studies, because expression of Orai3 may be affected by native proteins. The interference of expression seems confined to Orai Ca^{2+} channels, as mammalian STIM1 was also expressed and a response to 2-APB, albeit unexpected, was observed.

Contents

List of Figures

List of Tables

Acknowledgement

I would like to extend my thanks to some of the individuals who made the completion of this thesis possible. I'll begin by first thanking God. Were it not for His constant guidance and support, I think I would have lost my mind during the past couple of months. So, thank you Lord for being there, when I refused to let anyone else.

I would also like to thank my thesis director, J. Ashot Kozak, Ph.D., for not only the opportunity to work on this project, but also his tireless work revising, and revising, and revising, and revising this thesis. Were it not for his guidance, a lesser work would be presented before you today. I'll also take this opportunity to thank my committee members, all of you have, in some small (or large) way, helped make the completion of this project a less stressful undertaking. I truly appreciate all you've done to help. I'd also like to thank Dan Halm, Ph. D., and his wife Susan who have not only allowed us to use equipment, but provided me and my wife with the most awesome blankets known to man. Hand-made no less.

Finally, I'd like to thank my magnificent wife Laura, for putting up with my insane demands for the past few months; requests like keeping five and less-than-one year olds quiet so that I'd be able to work at home when necessary. I appreciate all you've had to sacrifice this past year, and want you to know that without you, and your support, I'd never have made it this far. "Thank you" doesn't even come close to making up for it, so we'll just have to figure something else out. :-)

Dedicated to

my exceptionally magnificent wife,

Laura Bennett.

Introduction

Two key articles published in the 1980's defined the new phenomenon of store-operated calcium entry (SOCE): Streb et al. (41) showed that stimulation with inositol (1,4,5)-trisphosphate (IP3) triggered calcium (Ca^{2+}) release from the endoplasmic reticulum (ER) and soon after, Putney (33), proposed that depletion of intracellular Ca^{2+} concentration ($[Ca^{2+}]_i$) signaled the plasma membrane Ca^{2+} entry channels to open (42). These and other early studies (17, 52) formed the framework for subsequent investigations of SOCE in various cell types. Initially, the more popular term used was capacitive calcium entry (CCE). Over 20 years later, other major players in this story were revealed. Stromal interaction molecule 1 (STIM1), was found to affect SOC influx in an RNA interference (RNA_i) based screen and identified as the ER calcium sensor (35, 22, 51). Shortly thereafter the store-operated calcium channel, Orai1, was identified (14, 31, 44, 50, 39).

There are two mammalian homologs of Orai1 – Orai2 and Orai3 – whose functions are not yet fully understood (35, 44, 42, 39). It is possible that Orai2 and Orai3 are expressed in a tissue-specific manner. This seems to be the case with estrogen receptor-positive (ER+) breast cancer cells, which have been shown to use Orai3 as their store-operated Ca^{2+} channel (29, 10). The demonstrable involvement of Orai3 in a disease state as prevalent as breast cancer, underscores the importance of further studies of these Orai channels whose function in the body is not yet understood. The presented study sets the foundation for pharmacological characterization of the Orai3 Ca^{2+} channel, using *Drosophila* S2 cells as a heterologous expression system. This system is expected to be of more general use for

physiological and pharmacological studies of all Orai channels. We begin by introducing calcium signaling through store-operated channels in non-excitable cells.

1.1 Background

1.1.1 Calcium Signaling

Ca^{2+} is an incredibly versatile signaling molecule, affecting all parts of the cellular signaling machinery. Ca^{2+} signaling is critical to such processes as exocytosis, transcription, cardiac function, mitosis and apoptosis (4, 5, 16, 39). The speed of these processes range from seconds to days (4).

Since Ca^{2+} can enter the cell's cytoplasm by influx at the plasma membrane or release from internal stores, such as those within the ER (4, 5, 39), it is necessary to maintain a balance between the two pathways. This is to prevent Ca^{2+} from accumulating where it should not, which would activate or deactivate cellular processes at inopportune times. Ca^{2+} concentration is regulated through activation of different ion channels. The most studied Ca^{2+} ion channels in the ER are the IP3 and ryanodine receptors (IP3R, RYR) (5, 21, 34). These channels are activated by second messengers.

"On" mechanisms are the means by which Ca^{2+} is released from internal stores into the cytoplasm. "On" mechanisms depend on Ca^{2+} channels (5) which may be voltage-operated channels (VOCs), receptor-operated channels (ROCs), and/or store-operated channels (SOCs) (5).

"Off" mechanisms also exist to quickly lower $[Ca^{2+}]_i$, and this is done through various pumps and exchangers (5). The plasma membrane Ca^{2+}-ATPase and Na^{+}/Ca^{2+} exchanger (if present) move Ca^{2+} out of the cell, while the sarco-endoplasmic reticulum Ca^{2+} ATPase (SERCA) will pump Ca^{2+} back into the ER, replenishing the cell's internal stores (5).

Orai1, the recently identified Calcium-Release Activated Calcium (CRAC) channel,

is a store-operated Ca^{2+} channel (31, 44, 14, 50, 39). Orai3 is closely related to Orai1 (14, 42, 16), and is thought to be involved in store-operated calcium entry (SOCE). According to the Basic Local Alignment Search Tool (BLAST), Orai3 has 58% nucleotide sequence homology with Orai1. When SOCs open they allow Ca^{2+} into the cytosol. This leads to $[Ca^{2+}]_i$ increasing from nanomolar to micromolar levels (5). This Ca^{2+} is both stimulatory and inhibitory (5) since this ion acts as a signal for such a wide array of cellular processes. Spatial regulation becomes very important in allowing for control of stimulatory and inhibitory Ca^{2+}-dependent mechanisms. Ca^{2+}-binding proteins act as buffers and allow the cell to control the local $[Ca^{2+}]_i$. Cytosolic Ca^{2+} buffers such as parvalbumin, calbindin-D, and calreticulin, along with Ca^{2+} pumps and exchangers are important in regulation of $[Ca^{2+}]_i$ (5). The affinity which these buffers have for Ca^{2+} is also important. Parvalbumin, for example, has a high affinity for Ca^{2+} but slower binding kinetics than calbindin-D and calreticulin (4). The different Ca^{2+} binding affinities allow for buffers which can modify amplitude, recovery time and diffusional range of Ca^{2+} (4).

In addition to their buffering capacity, cytosolic Ca^{2+} binding proteins can also act as Ca^{2+} sensors (5). Ca^{2+} sensors, such as troponin C, calmodulin, phospholipase C and recoverin respond to changes in $[Ca^{2+}]_i$. They do so with the aid of EF hand motifs and will bind Ca^{2+} to undergo conformational changes, and then activate downstream processes (5). This mechanism of detecting changes in $[Ca^{2+}]_i$ should be emphasized, as it will become relevant for another player in the SOCE mechanism, STIM1.

1.1.2 Store-Operated Calcium Entry

SOCE is an interesting, yet simple process. Broken down to its simplest form, it is a process which signals for Ca^{2+} to be allowed into the cell when more is needed (33, 5, 21). SOCE is triggered by the loss of Ca^{2+} from the cell's own internal ER Ca^{2+} stores. ER Ca^{2+} sensors detect the loss of Ca^{2+}, migrate close to the plasma membrane (PM), and signal PM Ca^{2+} channels to open. This further increases the $[Ca^{2+}]_i$ and allows for replenishing the stores

(42), as well as providing Ca^{2+} necessary for various cellular processes (4, 5, 16, 39).

Store-operated Ca^{2+} channels in lymphocytes are responsible for Ca^{2+} entering from extracellular fluid (i.e. blood) (21, 5, 16), and lack voltage-sensitive Ca^{2+} channels (23). T-cell receptor engagement activates the enzyme phospholipase C gamma (PLC_γ). PLC_γ will then hydrolyze phosphatidylinositol 4,5-bisphosphate (PIP2) in the membrane resulting in soluble IP3, and membrane-bound diacylglycerol (DAG) (5, 21). IP3 binds to IP3R opening it and allowing Ca^{2+} out of the ER down its concentration gradient (39, 42, 21). The emptying of ER Ca^{2+} stores is detected by STIM1 and leads to opening of the store-operated Ca^{2+} channels in the PM (detailed below) allowing Ca^{2+} into the cytosol (39, 42). This sustained Ca^{2+} influx is necessary for gene transcription driven by nuclear factor of activated T-cells (NF-AT) (43, 5, 21, 16). NF-AT, a transcription factor, is activated when an immune response is necessary, and drives transcription of the IL-2 gene (43, 21, 16). The importance of Ca^{2+} to this process is a result of NF-AT's dependence on calcineurin for activation.

The Ca^{2+} influx triggered by SOCE results in Ca^{2+} and calmodulin binding to the protein phosphatase calcineurin, activating it. Activated calcineurin then dephosphorylates NF-AT, allowing it to move into the nucleus (43, 2). Once inside the nucleus, NF-AT is able to bind the promoter region of interleukin and proliferation genes enabling their transcription, in effect triggering immune response (43, 5, 16). Notice that for efficient NF-AT activation, the Ca^{2+} elevation needs to be sustained, lasting 1-2 hours (43, 5, 21).

1.2 STIM1

Stromal interaction molecule 1 (STIM1), initially discovered as a membrane protein (45), was shown to be the Ca^{2+} sensor within the ER (35, 22, 51, 39). The related STIM2 and *Drosophila* STIM (*dStim*) were also discovered later (45). STIM1 and STIM2 are single-pass transmembrane proteins (16). Both are ER membrane localized proteins, until

emptying of the ER Ca^{2+} store causes translocation into, or close to, the PM (16).

STIM1 functions as a Ca^{2+} sensor by binding Ca^{2+} with its EF hand (45, 22), a motif also present in cytosolic Ca^{2+} sensors (see above). Upon Ca^{2+} depletion, ER-localized STIM1 will migrate to sites at or near the PM and bind Orai1, activating the channel. Once activated, Orai channels permit the flow of Ca^{2+} into the cell. To date, only Orai1 has been shown to be both necessary and sufficient for Ca^{2+} entry (14, 39). STIM2, a homolog of STIM1, was found by one group to be an inhibitor of STIM1-mediated SOCE (40). *dStim*, the *Drosophila* homolog of STIM1, is also an important regulator of SOCE and is involved in cell fate specification and tissue patterning (13).

1.3 Orai3

As mentioned above, Orai3 is a homolog of Orai1, the long sought after CRAC channel (14, 16). Even now, years after its discovery, the field still has a poor understanding of Orai3's native function and this is why studying Orai3 is important.

Though Orai channels behave similarly as Ca^{2+} entry channels, they have a different pharmacological profile. In mammalian cells, for example, interaction with the drug 2-aminoethoxydiphenyl borate (2-APB) generates different cellular responses depending on the protein to which it binds. While Orai1 will see slight activation upon introduction of $<$ 10 μM 2-APB, higher concentrations result in deactivation (14, 15, 31, 49), and blockade of SOCE. In contrast, Orai3 is activated by 2-APB concentrations of and above 50 μM 2-APB (15, 49). These contrasting responses will be exploited in this study.

The Orai family of proteins displays a wide expression profile, which includes T-cells and kidney (16). In HEK293 cells, knock down of Orai1 using siRNA reduced SOCE (16). Knock down of Orai2 or Orai3 did not significantly affect SOCE, however (16). These experiments in HEK cells are suggestive of Orai1's importance in initiating SOCE. As long as Orai1 is present in the membrane, SOCE will take place normally. Overexpression

experiments of Orai1 showing Ca^{2+} influx lasting minutes support this idea (16, 49). Ca^{2+} influx on the order of hours is necessary for gene transcription, however (2).

Expression of Orai3 and STIM1 in T-cells from severe combined immunodeficiency (SCID) patients results in marginal increases in SOCE, far lower than when Orai1 and STIM1 are overexpressed (16). In SCID patient fibroblasts only Orai3 contributed to a minor increase in SOCE over basal levels (16). Orai2 and STIM1 expression did not result in any increase over the basal SCID T-cell levels. These experiments indicate that while Orai2 and Orai3 are, at some level, capable of supporting SOCE, in these human cell types they are not the primary mediators of SOCE.

These results may be taken to suggest that Orai3 is potentially important to SOCE in cell types that do not rely on Orai1 for sustained Ca^{2+} levels, as T-cells do. An example of this has been displayed for ER+ cancer cells (29). This supports our belief that Orai3 is an important target of scientific inquiry, and that finding approaches to ease its study is a relevant and valuable endeavor. We begin this process by attempting to create a model system for studying pharmacological effects on Orai3.

1.4 *Drosophila* S2 cells

Drosophila cell line 2 (S2) has risen to prominence due to the ease of expressing proteins from other organisms in them. S2 cells have been used for both transient and stable expression of recombinant proteins (37). They are also easy to transfect and allow multiple copies of plasmid DNA to stably integrate into the genome (37). This property results in high levels of protein production which make them so attractive to use. The S2 cell line is derived from late stage *Drosophila* melanogaster embryos (38, 37). Schneider, the creator, described them as macrophage-like (37) and evidence for their immune lineage includes the following: (i) they support phagocytosis; (ii) produce antibacterial peptides; (iii) like mammalian macrophages prefer media with more carbonate, and (iv) will phagocytize other

dying S2s (37).

Another reason why S2 cells present an attractive target for protein expression is related to the possibility of finely regulating protein expression through the use of vectors with strong, inducible promoters (37, 47). An additional contributing factor for the use of S2 cells in this study was the expression of multiple homologs of Orai and STIM genes in mammalian cells. Humans have three Orais: Orai1, Orai2 and Orai3; and two STIMs: STIM1 and STIM2. In contrast, *Drosophila* cells have only one Orai (*dOrai*) and one STIM (*dStim*) isoform, but still carry out SOCE. Depletion of ER calcium is detected by *dStim* which signals for extracellular Ca^{2+} influx through *dOrai* in the PM (39).

The S2 cell population is known to display stable behavior over time (3). As with other immortalized cells, they can be frozen and used at later times. Another advantage is that it is possible to follow the responses of a population immediately after adding a drug (3). The expression of genes, either transiently or stably has been well documented. The silencing of gene function by RNA_i is also relatively simple and well characterized in these cells (35). All of these factors make the *Drosophila* Expression System (DES) very attractive to work with.

In our studies we will be introducing genes and testing their function. Ultimately, our goal is to generate stable cell lines expressing our mammalian genes, and use this system for the purpose of drug discovery. DES also allows for fine grained control of genes of interest (GOI) by using appropriate promoters to drive gene expression. We have selected the metallothionein promoter to drive expression of our GOIs in a regulated fashion. The introduction of mammalian ion channels and receptors using such a system has been demonstrated previously (37, 18, 1, 20, 30).

1.5 Metallothionein

The *Drosophila* metallothionein (Mtn) promoter is a strong inducible promoter (37, 7, 27, 47). Experimentally Cu^{2+} at concentrations $\geq$ 500 μM will strongly activate Mtn; with basal activity being reported as close to undetectable (37). At the concentrations of Cu^{2+} that will induce the Mtn promoter, S2 cells can grow and make proteins (37).

1.6 Chemical reagents used

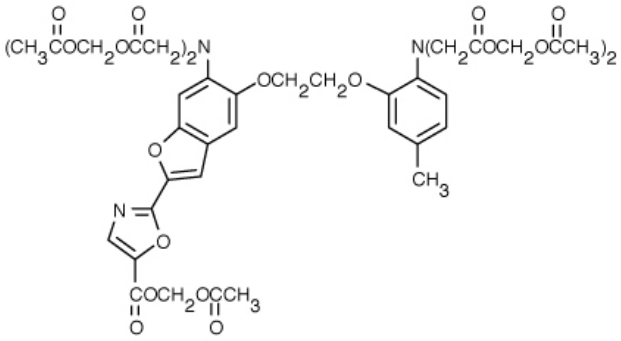

(a) Fura2-AM

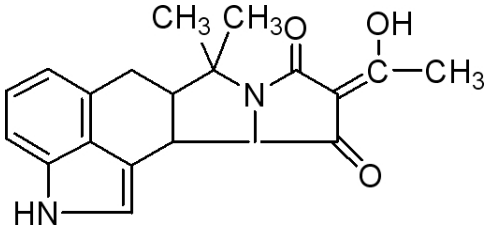

(b) CPA

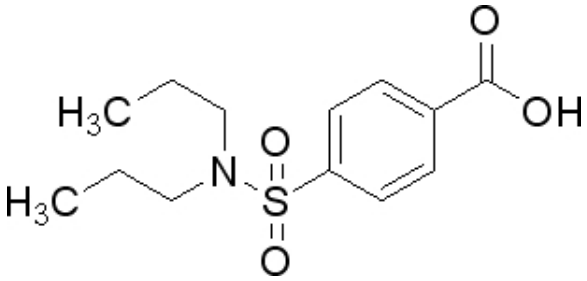

(c) Probenecid

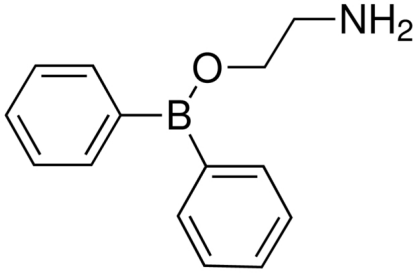

(d) 2-APB

Figure 1.1: Structures of chemical reagents used in this study.

1.6.1 2-Aminoethoxydiphenyl Borate

2-aminoethoxydiphenyl borate (2-APB) (CAS Number: 524-95-8, $(C_6H_5)_2BOCH_2CH_2NH_2$) is a drug which has multiple effects on a variety of cellular organelles. It is an inhibitor

of IP3Rs and SERCA pumps, and has both activating and inhibitory effects on channels (32, 6, 10). As mentioned above, its effect on Orai1 channels is to activate them at concentrations < 10 μM, while inhibiting at higher concentrations (32, 14, 16, 15). This dual effect is limited to Orai1, whereas for Orai3, 2-APB only activates at concentrations ≥ 50 μM (16).

Contrasting responses to 2-APB are often used to dissect functional differences in cells expressing multiple Orai isoforms (14, 15, 31, 49). There is precedent then for the use of 2-APB to help extract useful information about Orai3. Obtaining even more information on Orai3 through the use of 2-APB is possible. If interactions between Orai3 channels and 2-APB are direct, crystal structures with 2-APB could help define the structure of this binding site. Such information may be helpful in finding the natural modulator of Orai3's SOCE activating function. It is evident then, that the question of whether Orai3 interacts directly with 2-APB is worthy of study. By expressing Orai3 in a *Drosophila* expression system, it becomes possible to obtain enough protein to do the type of crystallographic studies mentioned above. This study then can provide the foundation for future structural investigation, and its utility is not limited to pharmacological studies.

1.6.2 Cyclopiazonic Acid

Cyclopiazonic Acid (CPA) (CAS Number: 18172-33-3, $C_{20}H_{20}N_2O_3$) is an inhibitor of the endoplasmic reticulum's Ca^{2+} ATPase (28). It has been shown to be specific for the SERCA pump, and has been shown not to affect other ATPases or calcium pumps (28). The affinity of CPA for its substrate is $\sim$120 nM. The use of CPA allows for manipulation of SERCA pumps and, by extension, the ER Ca^{2+} store content (34, chap. 2). Inhibition of the SERCA pump by CPA leads to release of the ER Ca^{2+} pools physiologically under the control of IP3R channels, (34, chap. 2). SERCA pump inhibition reveals a persistent Ca^{2+} leak from the ER, and makes it the predominant force driving Ca^{2+} movement. The result is an increase of cytoplasmic Ca^{2+} as it leaks from ER into cytoplasm. Ca^{2+} release occurs

relatively quickly (minutes), as CPA is membrane permeant (34).

CPA is added in a Ca^{2+} free solution containing a Ca^{2+} chelator. We then switch to a solution that contains Ca^{2+}, with no CPA. By emptying the cell's intracellular stores first, we may then reasonably assume that any subsequent increase in $[Ca^{2+}]_i$ is the result of Ca^{2+} entering the cell from the extracellular solution.

1.6.3 Ethylene glycol tetraacetic acid

Ethylene Glycol Tetraacetic Acid (EGTA) is a cation chelator with a preference for Ca^{2+} over Mg^{2+}, Na^{+} and K^{+} (19). It is used experimentally to bind available Ca^{2+} in the extracellular solution, making it unavailable for entry into the cell. This ensures that when $[Ca^{2+}]_i$ increases are observed during perfusion with an EGTA containing solution, we can assume that these increases are the result of intracellular Ca^{2+} release, and not extracellular Ca^{2+} entry (19, 34).

1.6.4 Fura-2

The ability to measure $[Ca^{2+}]_i$ changes comes from the use of Fura-2. Fura-2 is a calcium indicator whose ability to bind calcium is the result of a negatively charged tetracarboxylic acid core. It is a BAPTA derivative, which in turn, is a modification of EGTA (19, 34).

Fura-2 is a dual excitation indicator with a Kd of 145 nM for Ca^{2+}. At low $[Ca^{2+}]$ excitation peaks at approximately 370 nm, while binding Ca^{2+} changes the excitation peak to 340 nm. Emission, meanwhile, is monitored at 510 nm. This results in Ca^{2+} binding leading to an increase in fluorescence at 510nm, when Fura-2 is excited at 340 nm. There is a corresponding decrease in fluorescence at 510 nm, when excited at 380 nm if Ca^{2+} is bound. By exciting both wavelengths in quick succession, Ca^{2+} binding changes can be monitored. This is referred to as a ratiometric approach, and has advantages over single-wavelength excitation (discussed in ref.19).

The advantages are that the signal does not depend on the dye concentration, illumination intensity or optical path-length because we get normalized values from the ratios of the two wavelengths. Ratiometric measurements are therefore an improvement over the single-wavelength readings with respect to these issues as well. Dye leakage and photobleaching both lead to a loss of indicator during the experiment. In a single-wavelength setup, the dye concentration could gradually decrease, leading to a seeming decrease in Ca^{2+} signal. In the ratiometric setup, the effect of dye leakage or photobleached signals is mitigated by taking the ratios of these measurements. The ratios should remain constant regardless of the dye concentration or signal intensity. As an added advantage, ratiometric measurements increase sensitivity (19, 34).

One noteworthy drawback is that Fura-2 fluorescence can be quenched by Cu^{2+} (34, 27). Since we use $CuSO_4$ to induce gene expression in S2 cells, this is directly relevant to our study. Care therefore is taken with measurements from $CuSO_4$-induced S2 cells. These cells are spun down, washed in PBS, and then re-suspended in S2 media containing no $CuSO_4$ to minimize quenching.

Fura-2-AM

Ca^{2+} indicators are, necessarily, charged molecules. In spite of this, we need them to cross the lipophilic PM. Since diffusional transport of these large, charged molecules across the lipophilic membrane would be extremely slow, other methods are used to speed up the process. By esterification of the -COOH groups of Fura-2, these groups are made lipophilic and thus membrane permeant. Indicators with these modifications are usually available as acetoxymethyl (AM) esters. Such is the case here, and the Fura-2-AM variant is used to load the dye into our S2 cells. Once inside the cell, cytosolic esterases are needed to remove the AM groups. Once these groups are removed, Fura-2 regains its charge, and may no longer freely cross the PM.

One caveat of this method is that cell types with low esterase activity will display poor

loading (19). Another is that cellular processes, presumably designed to maintain ionic equilibrium, may pump the de-esterified, charged compound out of the cell. To combat this problem, the anion transporters responsible for this process can be blocked. This strategy was found to be necessary for S2 cells (9, 47). Probenecid was used for this purpose in our study.

1.6.5 Probenecid

Probenecid (CAS Number: 57-66-9, $C_{13}H_{19}NO_4S$) is a nonspecific inhibitor of anion transport (9, 25). The reason for wanting to inhibit anion transport is to prevent cells from transporting the Fura-2 dye out of the cytosol. Many cell types are capable of sequestering the dye into different compartments, and also of transporting the dye out of the cell (11). There are a number of methods proposed for how Fura-2's cytosolic concentration could be reduced (11, 9). Of those, the hypothesis that probenecid-sensitive anion transporters are responsible seems most plausible in *Drosophila* S2 cells (9). Murine macrophages have also shown a propensity for Fura-2 leakage (11). In the mouse macrophage model, the anion transporters were again implicated in Fura-2 leakage and blocking anion transport prevented Fura-2 sequestration and secretion (11). It is easy to see then that S2 cells, which are also of macrophage origin, would have a similar response (37).

Drosophila S2 cells have, in fact, been shown to exhibit poor loading of Fura-2, alleviated by probenecid (9). In our experiments we also experienced similar difficulties with loading the S2 cells in the absence of an anion blocker. Addition of 2.5 mM of probenecid alleviated this problem, increasing the number of cells loaded with Fura-2.

The mode of action of Probenecid

Probenecid is thought to act by inhibiting the clearance of ions (25). It has also been reported that the drug has non-specific effects on Ca^{2+} homeostasis (25). Such information

is important to be aware of, as Ca^{2+} measurements are the output from the experiments in our study. Care needs to be taken then, to ensure that the Ca^{2+} measurements would not be affected by probenecid. We address this by doing short 45-minute incubations in probenecid similar to other published studies (9, 35, 47), followed by washing these cells in our perfusion solution without probenecid.

Probenecid is soluble at basic pH. It is therefore dissolved in a solution of NaOH. This necessitates titrating the dye-loading solution back to the desired pH, after adding probenecid (11). In mouse macrophage experiments, no unexpected effects on cell viability after a *3-hour* incubation with probenecid were observed (11). While there are caveats to its use, incubation at room temperature and for short periods, does not appear to affect cell function or viability (9, 11, 48).

1.7 Specific Aims

Before attempting to characterize human Orai3 Ca^{2+} channels in *Drosophila* S2 cells, we needed to create the insect vector which contained our mammalian GOI. Standard molecular biology techniques were used to achieve this. The pharmacological characterization was done by measuring the effect of 2-APB on heterologously expressed Orai3. We hypothesized that gene expression of mammalian Orai3 in *Drosophila* S2 cells would result in functional Ca^{2+} channels that behave similar to those in mammalian cells expressing Orai3 genes, when treated with 2-APB.

1.7.1 Specific Aim #1

As mentioned earlier, *Drosophila* S2 cells provide a good system for expressing proteins from other organisms. The pucHygroMT vector was chosen to express our mammalian genes in S2 cells. Specific aim #1 is to create vector constructs using pucHygroMT which

express Orai3 and STIM1 in *Drosophila* S2 cells.

1.7.2 Specific Aim #2

After creating these vector constructs it will be necessary to determine if they are capable of supporting expression of the desired genes. Specific aim #2 is to show that we can successfully express heterologous genes in *Drosophila* S2 cells.

1.7.3 Specific Aim #3

It is our long term goal to ultimately use this system for drug discovery. For this to be possible we need to assess the effects which different drugs have in our system. This will be done using Ca^{2+} measurements taken in transiently transfected *Drosophila* S2 cells. Specific aim #3 is to determine whether 2-APB has the same effect on the heterologously expressed Orai3 in S2s that it has in mammalian cells. 2-APB is a pharmacological agent with defined effects on the Orai3 Ca^{2+} channel. By looking at the effect of 2-APB on heterologously expressed Orai3, we will be able to determine whether the model requires refinement, or is suitable as is.

1.8 Significance

As stated above, Orai3 Ca^{2+} channels have been implicated in a specific subset of breast cancer. It is tempting to envision a scenario where we can specifically target a type of breast cancer for treatment (10). This will require some method to test the efficacy of drugs being used, however. If successful, creating a model system in *Drosophila* has the possibility to simplify drug testing, and as a result speed the process up. This could benefit research of, not only breast cancer, but also other disease states involving SOCE. Cancers, such as leukemia, and even autoimmune diseases such as rheumatoid arthritis or lupus, arising

from defects of the immune system stand to benefit from this work.

A successful *Drosophila* expression system provides benefits to biochemical analysis of Orai channels as well. Techniques such as x-ray crystallography require large amounts of protein. Such quantities are not easily achieved when working with mammalian cells, but become feasible with a *Drosophila* expression system. This study is also significant as it opens the possibility for extending the body of knowledge on Orai channels in both functional and structural fields of research.

Materials and Methods

2.1 Materials

Table 2.1: List of Cloning Reagents

Manufacturer	Item	Location
5 Prime	PerfectPrep EndoFree Plasmid Maxi Kit	Gaithersburg, MD
	Agarose Gelextract Mini Kit	
Agilent Technologies	Easy-A One-Tube RT-PCR Kit	Santa Clara, CA
Sigma-Aldrich	TRI Reagent®	Louis, MO
Fermentas	DNase I, RNase-free	Glen Burnie, MD
IBI Scientific	Ethidium Bromide (EtBr)	Peosta, IA
Invitrogen	MAX Efficiency® DH10β Competent cells	Carlsbad, CA
Lucigen	2.5 mM dNTP Mix	Middleton, WI
	EconoTaq PLUS GREEN 2X Master Mix	
Promega	PureYield™ Plasmid Miniprep System	Madison, WI
Research Products	Agarose	Mount Prospect, IL
International (RPI)	Tryptone	
	Yeast Extract	
New England Biolabs	Antarctic Phosphatase	Ipswich, MA
	T4 DNA Ligase	
	Various restriction enzymes	

2.1.1 Restriction enzymes

The following is a list of the restriction enzymes used. All were purchased from NEB:(i) SalI; (ii) XbaI; (iii) BamHI; (iv) StuI; (v) XhoI; (vi) ApaI; and (vii) KpnI.

Table 2.2: List of PCR Cloning Primers

Primer	Sequence
Orai3 start salI	TGCCGAGTCGACATGAAGGGCGGCGAGGGG
Orai3 end xbaI	TGCCGATCTAGATCACACAGCCTGCAGCTCCCC
Stim1 start salI	TGCCGAGTCGACATGGATGTATGCGTCCGTC
Stim1 end xbaI	TGCCGATCTAGAGCCTACTTCTTAAGAGGCTTCTT

Table 2.3: List of RT-PCR Primers

Primer	Sequence	Size
orai3_rtpcr_fwd	GAGTGACCACGAGTACCCACC	
orai3_rtpcr_rev	GGGTACCATGATGGCTGTGG	508 bp
hstim1_end_fwd	TTGGATTCTTCCCGTTCTCACAGC	
hstim1_rev	GCCTACTTCTTAAGAGGCTTCTT	228 bp
rp49-fwd	ATCGGTTACGGATCGAACAA	
rp49-rev	GACAATCTCCTTGCGCTTCT	165 bp
HygBP3	CCTGAACTCACCGCGACGTCTGTCG	
HygBP4	AGGCAGGTCTTGCAACGTGACACC	303 bp

2.1.2 Primers

All primers were purchased from Integrated DNA Technologies (Coralville, IA).

Table 2.4: List of Cell Culture Reagents

Manufacturer	Item	Location
Atlanta Biologicals	Fetal Bovine Serum - catalog no. S11050	Lawrenceville, GA
Lonza	Schneider's Drosophila Medium	Walkersville, MD

2.1.3 *Drosophila* resources

Drosophila Schneider line 2 (S2) cells, the pucHygroMT plasmid and the puc18-act-gfp plasmid were all purchased from the Drosophila Genomics Resource Center (Bloomington, IN). Figure 2.1 shows a schematic of the pucHygroMT vector, with possible sites of insertion in the multiple cloning site (MCS).

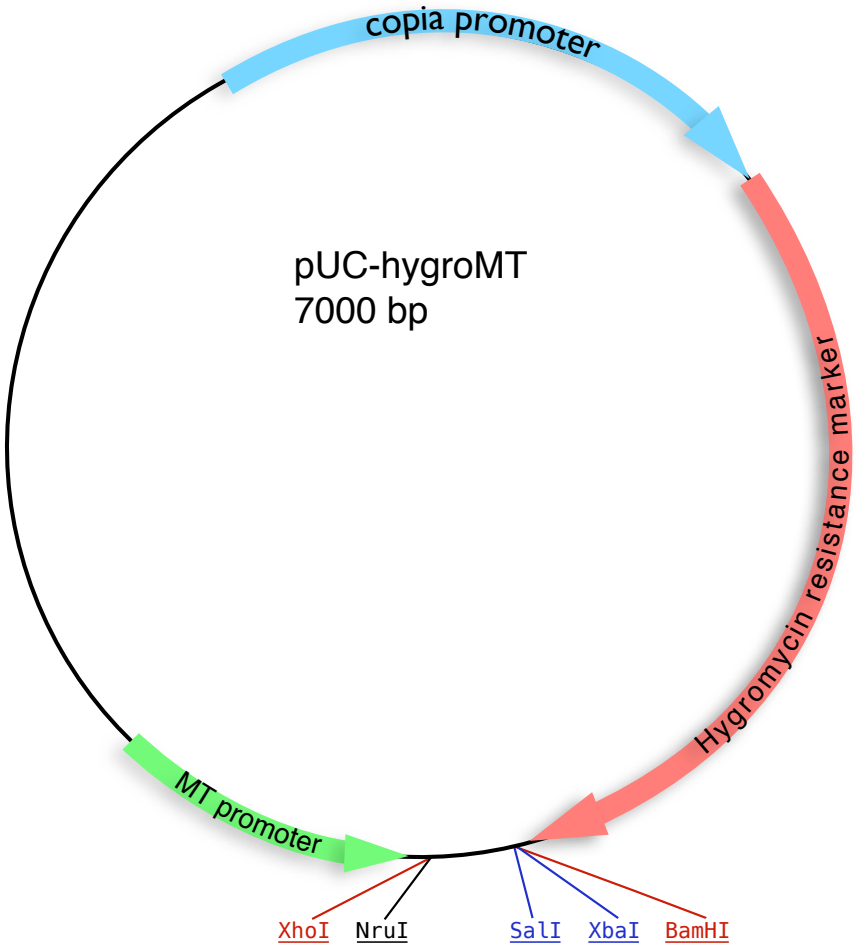

Figure 2.1: Map of the pucHygroMT vector. pucHygroMT contains `SalI` and `XbaI` sites which were used to insert both Orai3 and STIM1 into the MCS.

Table 2.5: List of Chemical Reagents

Manufacturer	Item	Location
Acros Organics	Ethylene Glycol Tetraacetic Acid (EGTA)	Geel, Belgium
	4-(2-hydroxyethyl)-1-piperazineethanesulfonic	
	acid (HEPES)	
	HEPES Sodium Salt (HEPES-Na)	
	Paraformaldehyde 96%	
	Sodium Chloride (NaCl)	
Fisher Scientific	Cupric Sulfate Pentahydrate ($CuSO_4 \cdot 5H_2O$)	Fair Lawn, NJ
	Dimethyl Sulfoxide (DMSO)	
	D-glucose	
	Hydrochloric Acid (HCl) 10N	
	Potassium Chloride (KCl)	
	Sodium Hydroxide (NaOH) 10N	
Invitrogen	Fura-2 AM	Carlsbad, CA
Mirus Bio LLC	*Trans*IT®-2020 Transfection Reagent	Madison, WI
MP Biomedicals	Agar	Solon, OH
	Probenecid	
Sigma-Aldrich	2-Aminoethyl diphenylborinate (2-APB)	St. Louis, MO
	Cyclopiazonic Acid (CPA)	
	Pluronic® F-127	
	Fluka Analytical 1.0 M $CaCl_2$	
	Fluka Analytical 1.0 M $MgCl_2$	

Table 2.6: List of Instruments

Manufacturer	Item	Location
Applied Biosystems	2720 Thermal Cycler	Foster City, CA
Denver Instruments	UltraBasic pH/mV meter	Bohemia, NY
Sutter Instrument	Lambda 10-B	Novato, CA
Thermo Fisher Scientific	NanoDrop ND 1000	Wilmington, DE
Intracellular Imaging Inc.	175 W Xenon Lamp	Cincinnati, OH
B & B Microscopes, Ltd.	Olympus CKX41 Inverted Microscope	Pittsburgh, PA

2.2 Methods

2.2.1 Maintenance of cell lines

Drosophila S2 cells were cultured at 27 °C in Schneider's *Drosophila* medium supplemented with 10% fetal bovine serum (FBS).

2.2.2 Creation of *Drosophila* expression constructs

Molecular Cloning

We needed to express human genes (Orai3, Stim1) on a *Drosophila* background, a process which required some molecular biology finesse. We chose to accomplish this by transferring these genes to a *Drosophila* vector. We selected the pucHygroMT plasmid as our vector, whereas Orai3 and Stim1 were the kind gifts of Dr. Stefan Feske, NYU School of Medicine.

pucHygroMT (see figure 2.1) contains a metallothionein promoter before the MCS, allowing one to induce the expression of genes placed in the MCS. It provides the necessary genes for driving constitutive hygromycin B resistance and, the use of this vector for induction and creation of stable lines has previously been documented (12).

Our genes of interest – human Orai3 and STIM1 – were ligated into the pucHygroMT plasmid using `SalI` and `XbaI` sites. The inserts for our genes of interest were created by polymerase chain reaction (PCR) using the primers listed in Table 2.2. The `Orai3 start salI` and `Orai3 end xbaI` primers were used for the Orai3 insert. The Stim1 insert was generated using `Stim1 start salI` and `Stim1 end xbaI` primers. The forward primer for each insert contained a `SalI` restriction site (**GTCGAC**), protected by the **TGCCGA** sequence. The reverse primer for each insert had an `XbaI` restriction site (**TCTAGA**), protected by the **TGCCGA** sequence.

Each PCR reaction consisted of: (i) 1X Easy-A reaction buffer; (ii) .2 mM dNTPs;

(iii) 2 μM forward; and (iv) 2 μM reverse primers; (v) 2 μL Easy-A PCR enzyme; (vi) 50-100 ng of template DNA; and (vii) nuclease-free water up to 100 μL.

The PCR reaction thermocycler parameters for each amplicon were as follows:

Orai3, (i) an initial denaturation step at 95 °C for 3 minutes; (ii) 27 cycles of denaturation at 95 °C for 40 seconds, followed by annealing at 65 °C for 30 seconds, then extension at 72 °C for 1 minute; and (iii) a final extension of 72 °C for 7 minutes.

STIM1, (i) an initial denaturation step at 95 °C for 3 minutes; (ii) 27 cycles of denaturation at 95 °C for 40 seconds, followed by an annealing step at 65 °C for 30 seconds, then extension at 72 °C for 130 seconds; and (iii) a final extension of 72 °C for 7 minutes were performed.

After the PCR reactions were completed, the amplicons were digested with `SalI` and `XbaI`, then ligated into a similarly digested pucHygroMT vector (see details below).

Engineering *Drosophila* vector contructs

Each PCR product and the pucHygroMT vector were digested by `SalI` and `XbaI` restriction enzymes. The vector digest was followed by treatment with Antarctic Phosphatase, according to the manufacturer's instructions. Phosphatase treatment removed the 5′ phosphate group at the end of the digested vector DNA. This helped prevent spontaneous recircularization and increased the amount of vector available to ligate with the insert. The digested vector and digested PCR amplicons were run on a 0.8% 1X TAE agarose gel for 90 minutes at 80 V. Following electrophoresis, the DNA band was excised under UV illumination. The vector and insert DNA were then purified using the Agarose GelExtract Mini kit. After purifying the DNA, a ligation reaction was performed with T4 DNA ligase following the manufacturer's specifications. The insert to vector ratios in the ligations were 9:1 (by volume). After a 15 minute incubation at 25 °C, the ligation mixture was used to transform DH10β competent cells. The ligated constructs were renamed to indicate the inserts, thus pucHygMT-Orai3 contained Orai3, while pucHygMT-STIM1 contained Stim1.

Transformation of ligated DNA

A 15 ml round-bottom tube was chilled on ice, prior to addition of 100 μL thawed DH10β cells. Subsequently, 4 μL of the ligation mixture was added, mixed gently by flicking, then chilled on ice for 30 minutes. Next, the tube was incubated at 42 °C for 45 seconds, then quickly transferred to ice for 90 seconds. After this, 900 μL of SOC medium was added. A one hour incubation at 37 °C followed, with shaking at 250 RPM. 200 μL of this transformation mixture was plated on LB-Agar plates containing 100 μg/mL of the antibiotic ampicillin (+Amp). The resulting LB-Agar +Amp plates were placed in an incubator at 37 °C overnight. After 16-18 hrs the plates were transferred to 4 °C. Individual colonies from these plates were used to start miniprep cultures and obtain plasmid DNA.

Minipreparation of plasmid DNA

Single colonies were picked and added to 4 ml of LB supplemented with 100 μg/mL of ampicillin. This mixture was placed in an incubator at 37 °C, with shaking at 250 rpm, for 16-18 hours. A miniprep procedure was performed according to the instructions provided with the Pureyield™ Plasmid Miniprep System. DNA concentrations were estimated using a NanoDrop ND 1000 spectrophotometer.

Maxipreparation of plasmid DNA

A maxiprep culture consisting of 100 ml of LB, supplemented with 100 μg/ml of ampicillin was started, using 100 μL of the miniprep culture. This mixture was placed in an incubator at 37 °C, with shaking at 250 rpm, for 16-18 hours. A maxiprep procedure was performed according to the protocol of the PerfectPrep EndoFree Plasmid Maxi kit. DNA concentrations were estimated using a NanoDrop ND 1000 spectrophotometer.

2.2.3 Transfection of S2 cells

S2 cells were transfected with *Trans*IT®-2020 transfection reagent according to the manufacturer's instructions. Briefly, one day prior to transfection, S2 cells were plated at 80% confluency in a 6-well tissue culture plate. pucHygMT-Orai3 vector transfections were done with 1 μg of DNA per well. Transfections involving pucHygMT-STIM1 used 2 μg of DNA per well. pucHygMT-STIM1 and pucHygMT-Orai3 co-transfections were performed at a 2:1 ratio (Stim1:Orai3).

As a positive control for transfection, 0.25 μg of the green fluorescent protein (GFP) vector puc18-act-gfp, was co-transfected with the above constructs. A ratio of 3 μL of *Trans*IT®-2020 was used per 1 μg of maxiprepped DNA.

Induction of transfected S2 cells with $CuSO_4$

Drosophila S2 cells were induced by the addition of 750 μM $CuSO_4$ one or two days post-transfection.

2.2.4 RT-PCR and cDNA synthesis

Total RNA was isolated from transfected S2 cells, two days post-induction, using TRI reagent® as per the manufacturer's instructions. Traces of contaminating DNA were removed using RNase-free DNase I. For each μg of RNA, 1 μL of DNase I was added. First strand cDNA synthesis was performed using the MMLV reverse transcriptase (RT). Briefly, 1 μg of mRNA was reverse transcribed into cDNA during a 30 minute incubation at 45 °C. This cDNA served as the template for successive PCR reactions.

The RT reaction mixture contained: (i) 1X MMLV buffer; (ii) .8 mM dNTPs; (iii) 1 μg of template RNA; (iv) 2 μL MMLV RT; and (v) nuclease-free water up to 50 μL. RT reactions were also performed on samples with the RT omitted – to determine whether any contaminating DNA was still present.

PCR reactions were performed in a 2720 Thermal Cycler. The *Drosophila* housekeeping gene, ribosomal protein 49 (rp49), was used as a positive control to determine whether cDNA was made in the preceding RT reaction (7, 24).

Each PCR reaction contained: (i) 1X Easy-A reaction buffer; (ii) .3 mM dNTPs; (iii) 1 μM forward; and (iv) 1 μM reverse primers; (v) .5 μL Easy-A PCR enzyme; (vi) 5 μL of cDNA template from the (no-)RT reaction; and (vii) nuclease-free water up to 50 μL. The sequences of these RT-PCR primers (24, 26, 46), and expected band sizes are given in Table 2.3.

The PCR reaction parameters are as follows:

Orai3 and STIM1, (i) an initial denaturation step at 95 °C for 3 minutes; (ii) 30 cycles of denaturation at 95 °C for 30 seconds, then annealing at 55 °C for 30 seconds, then extension at 72 °C for 1 minute; and (iii) a final extension of 72 °C for 10 minutes was performed.

HygBP, (i) an initial denaturation step at 95 °C for 3 minutes; (ii) 30 cycles of denaturation at 95 °C for 30 seconds, then annealing at 65 °C for 30 seconds, then extension at 72 °C for 30 seconds; and (iii) a final extension of 72 °C for 10 minutes was performed.

rp49, (i) an initial denaturation step at 94 °C for 3 minutes; (ii) 30 cycles of denaturation at 94 °C for 45 seconds, then annealing at 50 °C for 1 minute, then extension at 72 °C for 1 minute 30 seconds; and (iii) a final extension of 72 °C for 7 minutes was performed.

2.2.5 Ca^{2+} imaging experiments

Two primary solutions were used for the Ca^{2+} imaging experiments. The first, designated **2 Ca**, contained (in mM): 2 $CaCl_2$, 4 $MgCl_2$, 150 NaCl, 5 KCl, 10 HEPES and, 10 D-glucose at pH 7.2 (51). The second solution **1 EGTA**, contained (in mM), 1 EGTA, 6 $MgCl_2$, 150 NaCl, 5 KCl, 10 HEPES and, 10 D-glucose at pH 7.2 (51). The dye loading solution referred to below was comprised of 2 Ca, 0.02% Pluronic F-127, 2.5 mM probenecid and 4 μM Fura2-AM.

Cytosolic Ca^{2+} signals were measured in the following way: S2 cells, cultured at 27 °C, were plated on 35 mm glass-bottom chambers made by J. Ashot Kozak, Ph. D. The cells were allowed to adhere for 30 minutes at room temperature, the old medium was removed, and the cells washed in 1X DPBS twice. After the wash, the dye-loading solution was added to the attached cells and they were incubated at room temperature for 45 minutes. The cells were then washed twice with the 2 Ca solution, and used for imaging.

Ca^{2+} imaging was performed on the stage of an Olympus CKX41 inverted microscope. Cells were perfused at a rate of approximately 4 mL/min using the solutions indicated in the figures below. Loaded cells were exposed to light of 340 nm and 380 nm wavelengths, and emitted light at 510 nm was recorded by the InCytIM 2 imaging system (Intracellular Imaging, Cincinnati, OH) installed on a Dell Optiplex 745C computer. The UV light source was a 175 W Xenon arc lamp. The wavelengths were selected using filters in the Lambda 10-B SmartShutter which was controlled by the InCytIM 2 software.

Selection of data for analysis

The traces were selected based on the following criteria: (i) there was a visible response to CPA introduction; (ii) the initial perfusion with 2 Ca was relatively stable over time; (iii) the absolute values of the measurements at 340 nm and 380 nm were $\geq$ 40 during initial perfusion with 2 Ca; and (iv) the 340 nm and 380 nm recordings mirrored each other as time progressed.

Statistical analysis of imaging experiment data

Error bars shown on the traces depict the standard error of the mean. Area under the curve analysis was performed using Origin 8 software. Statistical analysis of the area under the curve data was performed using one way ANOVA with SAS software. Differences were considered significant if p values were < 0.05. The p values of < 0.0001 were denoted by the *** characters.

Results

3.1 Creating inducible vectors

Orai3 and STIM1 inserts were created as indicated in the methods. The inserts and pucHygroMT vector were then digested to facilitate ligation. After ligation of pucHygroMT and inserts and transformation, DNA obtained by maxipreparation was digested to confirm that the desired constructs were generated. These results of these digests are given below.

Figure 3.1 shows the results of digesting the pucHygMT-Orai3 construct after electrophoresis on a 0.8% agarose gel. The marker lane, shows DNA bands of known sizes, used for estimating the sizes of bands in experimental lanes. Lane 1 shows bands obtained when both pucHygroMT vector and the Orai3 PCR amplicon are digested with `SalI`+`XbaI`. The pucHygroMT vector map gives its size as 7000 bp. Based on comparison with the DNA marker, doubly digested pucHygroMT is estimated to be $\sim$7000 bp. This implies a difference of only a few bases between the `SalI` and `XbaI` sites in the MCS. The Orai3 PCR amplicon, after digestion, is 894 bp. This comes from the 888 bp size of Orai3, plus the bases for the digested `SalI` and `XbaI` restriction sites. The size of pucHygMT-Orai3 is estimated to be 7888 bp. This comes from the $\sim$7000 bp size of the digested vector and the 888 bp Orai3 insert (restriction sites in the Orai3 amplicon are not added to the total, as they are already accounted for in the vector).

We tested if the insertion of pucHygMT-Orai3 was successful by performing restriction digests and comparing the sizes of the obtained bands to the calculated size. The dou-

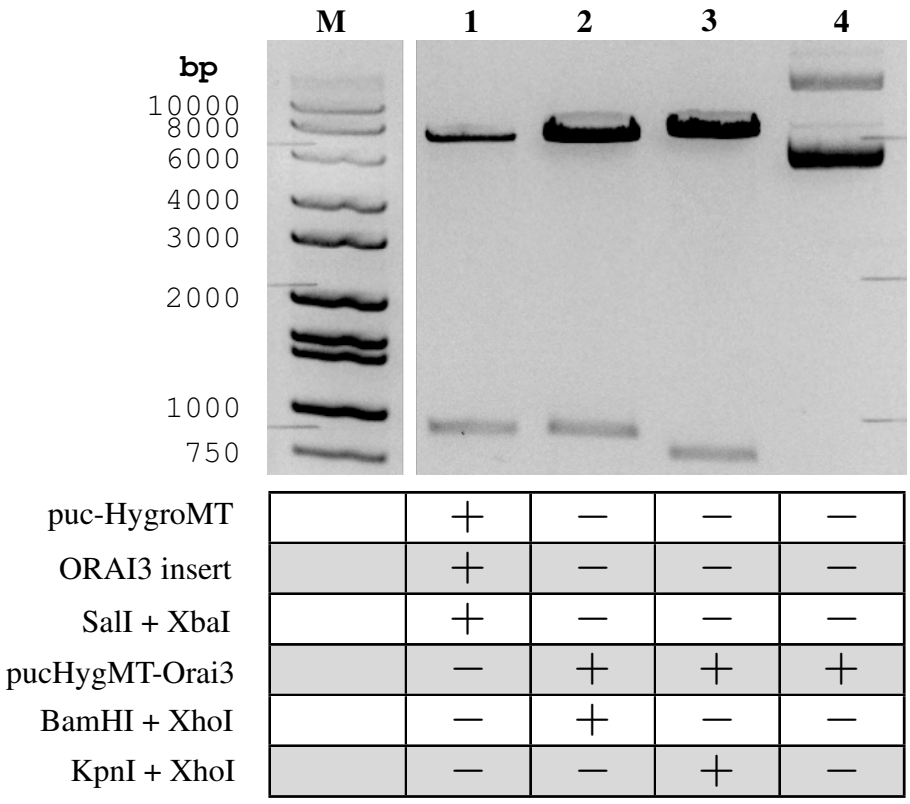

Figure 3.1: Restriction digests confirm the insertion of Orai3 into puc-HygroMT. **Lane M** shows the DNA ladder, with the sizes of the corresponding bands to their left. **Lane 1** shows a `SalI+XbaI` double digest of both pucHygroMT and the Orai3 PCR amplicon. The double digested pucHygroMT, ∼7000 bp in size, is the higher of the two bands. Orai3, which is 894 bp in size, is the lower band. **Lane 2** shows the result of a `BamHI+XhoI` double digest of pucHygMT-Orai3. The complete vector is ∼7888 bp, giving a 931 bp fragment and the remainder of the vector, ∼6957 bp. **Lane 3** shows the result of a `KpnI+XhoI` double digest of pucHygMT-Orai3. This gives a 796 bp band and a remaining ∼7092 bp band. **Lane 4** shows the undigested pucHygMT-Orai3, yielding supercoiled and open circular DNA species.

ble digest of pucHygMT-Orai3 with `BamHI` and `XhoI` is shown in lane 2 of Figure 3.1. Digestion with these enzymes is expected to yield a 931 bp and ∼6957 bp bands. Observed bands are approximately this size, based on comparison with our DNA marker, and the digested DNA in lane 1. Our 931 bp band is at roughly the same point as the 894 bp Orai3 insert, both just below the 1000 bp mark.

To test if the insertion was in the correct orientation, we digested with one enzyme

that cut in the vector backbone, and another that cut in the insert. Lane 3 of Figure 3.1 shows the result of a KpnI and XhoI double digest of pucHygMT-Orai3. Here we see the ∼7888 bp vector producing the expected 796 bp and ∼7092 bp bands. The last lane shows undigested pucHygMT-Orai3. We are therefore able to observe the supercoiled and open circular DNA species of the vector in lane 4 (36). In summary, Figure 3.1 shows that Orai3 was inserted into pucHygroMT, and more importantly, in the correct direction. Further confirmation was obtained after direct sequencing of pucHygMT-Orai3.

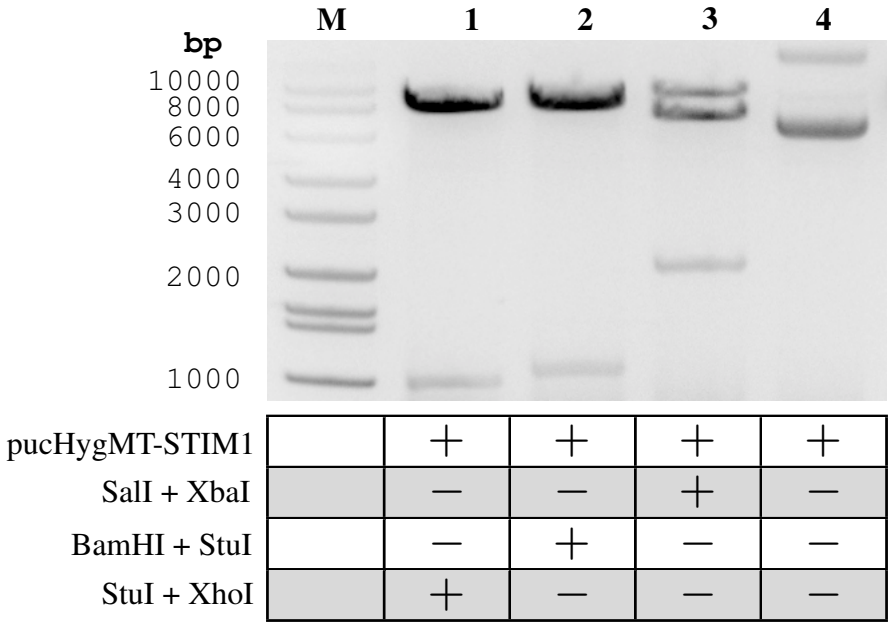

Figure 3.2: Restriction digests confirm the insertion of STIM1 into puc-HygroMT. **Lane 1** shows a `StuI+XhoI` digest of pucHygMT-STIM1. The ∼7000 bp pucHygroMT and 2060 bp STIM1 create a ∼9060 bp construct. `StuI+XhoI` digestion gives 1016 bp and ∼8044 bp bands. **Lane 2** shows the result of a `BamHI+StuI` digest of pucHygMT-STIM1. This yields 1087 bp and ∼7973 bp bands. **Lane 3** is the `SalI+XbaI` digest of pucHygMT-STIM1. A 2066 bp band and a ∼6994 bp band are the result. Linearized pucHygMT-STIM1, at ∼9060 bp is also present. **Lane 4** shows the undigested pucHygMT-STIM1. We see supercoiled and open circular vector DNA species here.

We again confirmed successful creation of a STIM1 construct with restriction digests. Figure 3.2 shows the results of pucHygMT-STIM1 digests after electrophoresis on a 0.8% agarose gel. Again, the marker lane shows DNA of known sizes, and is used to estimate the band size in other lanes.

In lane 1 the `StuI+XhoI` digest provides confirmation of STIM1 insertion into pucHygMT-STIM1. The `StuI` site is specific to STIM1 while the `XhoI` site is specific to the vector backbone. Two bands, sized at ∼8044 bp and 1016 bp were expected and observed. In lane 2, the `StuI` and `BamHI` digest provide additional confirmation of properly inserted STIM1. In this reaction the `BamHI` site is present in the vector. This digest yields the anticipated bands at ∼7973 bp and 1087 bp. Insertion of STIM1 in the reverse direc-

tion would have yielded different sizes. For example, the StuI+XhoI digest would have yielded 1116 bp and ∼7944 bp, making the smaller band visibly higher than 1 kb. These results confirm that our insert is present in the correct orientation. We can see that our gel is also able to resolve the difference between 1016 bp and 1087 bp (though not between 1016 bp and 1000 bp) providing further evidence that our inserts are oriented correctly.

The SalI and XbaI digest in lane 3 further supports our claims. The 2066 bp STIM1 and ∼6994 bp vector fragments are visible. A third band, the linearized pucHygMT-STIM1 vector, is also visible at ∼9060 bp. That the ∼8 kb (7973 bp) band in lane 2, fits between our expected ∼7 kb and ∼9 kb bands in lane 3 also supports our assertion that pucHygMT-STIM1 contains STIM1 in the desired orientation. Lane 4 shows undigested pucHygMT-STIM1 with supercoiled and open circular DNA species (36).

3.2 Demonstrating inducible expression

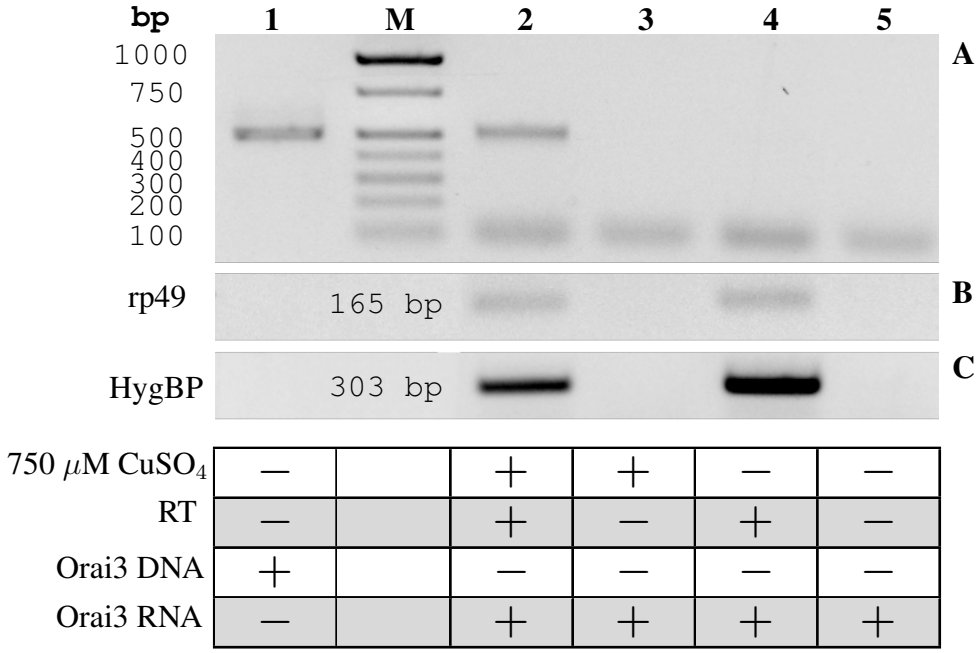

Figure 3.3: Inducible Orai3 expression *Drosophila* in S2 cells. (**A**) In **lanes 1-5** the Orai3 RT-PCR primer pair are used (see table 2.3) **Lane 1** shows the band from a positive control PCR reaction. Orai3 DNA is used as the template. **Lanes 2-5** show RT-PCRs using RNA from isolated pucHygMT-Orai3 transfected S2 cells. **Lanes 2-3**: S2 cells were induced with 750 μM $CuSO_4$. 508 bp band only present when RT is added. **Lane 4-5**: S2 cells were not induced with $CuSO_4$. No band present after RT-PCR. (**B**) RT-PCR of the same samples as in A, using rp49-specific primers. rp49 band at 165 bp is only seen in RT containing reactions. (**C**) RT-PCR of the same samples as in A, with HygBP-specific primers. HygBP bands at 303 bp are seen only in reaction where RT was added.

The RT-PCR reactions in Figure 3.3 were performed with total RNA collected from pucHygMT-Orai3-transfected (Orai3+) S2 cells. Figure 3.3 shows that induction of Orai3 RNA in these S2 cells is successful. Panel A shows that DNA positive control and RNA induction bands are the same size, 508 bp. No observable band is present when $CuSO_4$ was not added to Orai3+ S2 cells (lanes 4 and 5). This suggests negligible levels of Orai3 gene expression when under control of the metallothionein promoter.

Panel B shows rp49 RNA present in equal amounts for Orai3+ cells with or without $CuSO_4$. The rp49 RT-PCR measures the expression of the housekeeping gene rp49, and

serves as a positive control for RT-PCR of S2 RNA. Panel C shows more HygBP RNA in Orai3+ S2 cells with no $CuSO_4$ added. This is suggestive of a pipetting error. Panels A, B and C all showed no evidence of DNA contamination of these RT-PCR reactions, since omission of RT resulted in lack of visible signal.

Some lower bands were observed in the RT-PCR reactions and are likely the result of primer-dimer products. Such phenomena have been documented elsewhere (8).

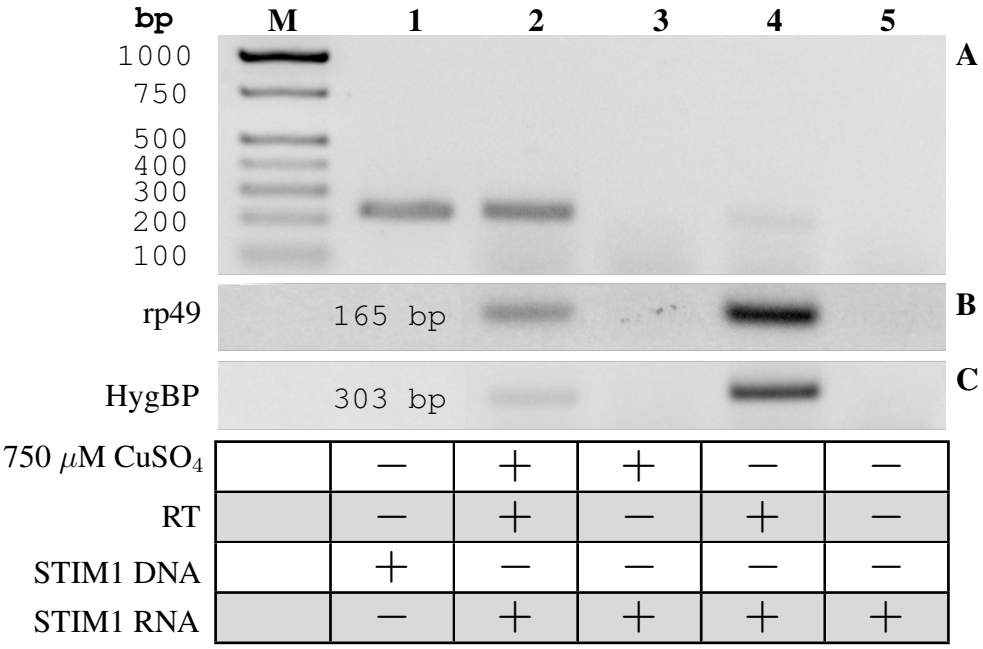

Figure 3.4: STIM1 expression is inducible in *Drosophila* S2 cells. (**A**) In **lanes 1-5** the STIM1 RT-PCR primer pair are used (see table 2.3). **Lane 1** shows the positive control PCR band using STIM1 template DNA. **Lanes 2-5** show RT-PCRs using RNA from isolated puc-HygMT-STIM1 transfected S2 cells. **Lanes 2-3**: S2 cells induced with 750 μM $CuSO_4$. 228 bp band present only when RT added. **Lanes 4-5**: S2 cells not induced with $CuSO_4$. Faint band at 228 bp seen when RT added. (**B**) RT-PCR using rp49-specific primers yields bands only in lanes containing RT. (**C**) RT-PCR using HygBP primers yields bands only in lanes containing RT.

The RT-PCR reactions in figure 3.4 were performed on total RNA collected from puc-HygMT-STIM1-transfected (STIM1+) S2 cells. Figure 3.4 shows that induction of STIM1 RNA in these S2 cells is successful. Panel A shows that DNA positive control and RNA induction bands are the same size. Both show up in the region where we would expect to see a 228 bp band. A faint band in the uninduced STIM1 RT-PCR reaction is visible in lane 4 of panel A. This suggests a basal level of expression for STIM1 when under the control of the metallothionein promoter.

Panels B and C show that more RNA was present in RT-PCR reactions of uninduced STIM1+ S2 cells, when compared to RNA from $CuSO_4$ induced STIM1+ S2 cells. This is seen in panels B and C, suggesting an error in estimating the RNA concentration using

the NanoDrop spectrophotometer. This adds further support for the successful induction of STIM1 RNA from $CuSO_4$ induced STIM1+ cells: more starting RNA was present in the *uninduced* RT-PCR reactions, yet a much brighter STIM1 band was present in the induced lane.

There was no evidence of DNA contamination of these RT-PCR reactions. Negative control lanes without RT had no bands.

3.3 Effective measurement of Ca^{2+} transients

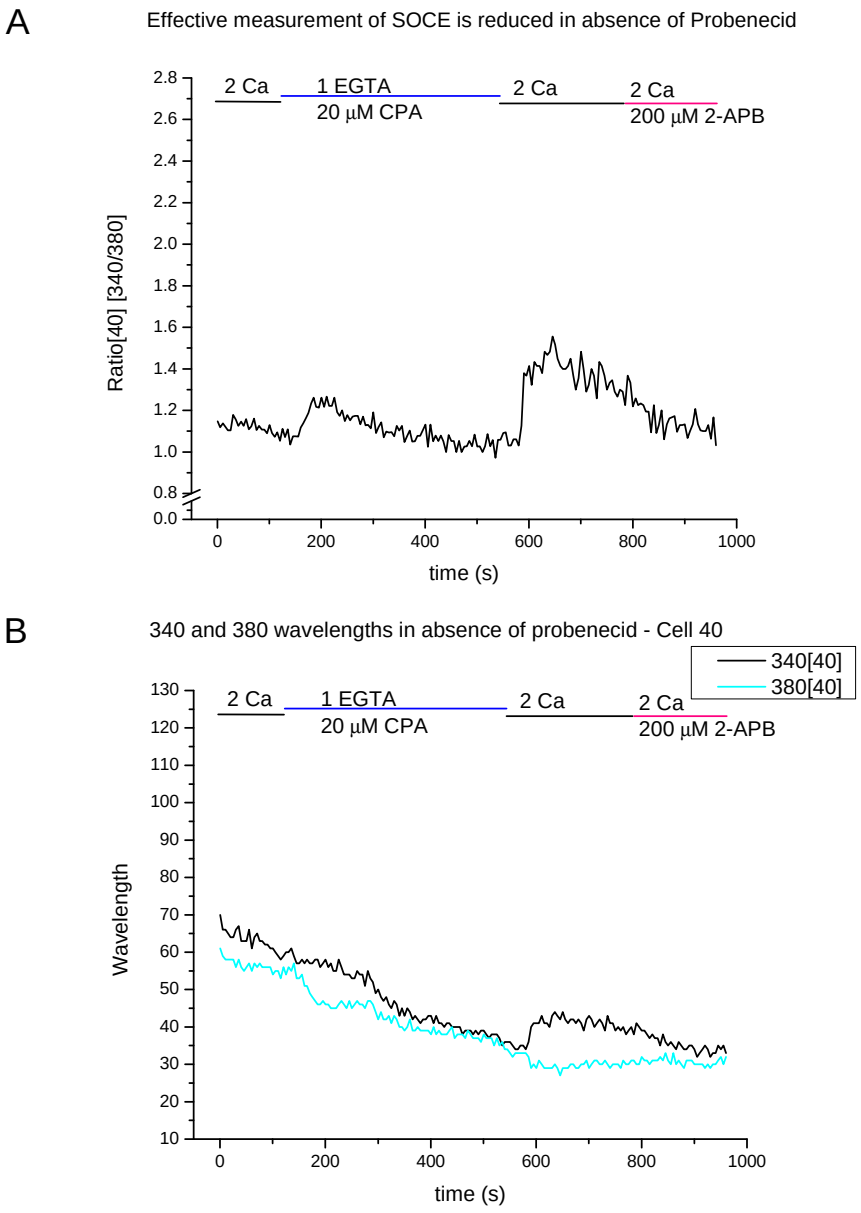

Figure 3.5: The absence of probenecid results in less efficient dye loading in S2 cells. (**A**) The ratio of the 340 nm and 380 nm wavelengths of an individual cell during the course of one perfusion experiment where probenecid was omitted from the incubation solution. (**B**) The individual 340 nm and 380 nm wavelength values, which produced the ratio seen in **A**.

Figure 3.5A shows a recording from an individual S2 cell loaded without probenecid being present in the dye-loading solution (DLS). Figure 3.5B shows the individual 340 and 380 nm wavelength values that produced the trace in A. Though the trace of the ratio hides it, we see that both wavelengths values start decreasing immediately after the start of the experiment. The decreasing values continue to the end of the experiment. The decay likely reflects leakage of Fura-2 which takes place in S2 cells if probenecid is absent in the DLS (11). The Ca^{2+} ratios reported after SOCE, upon reintroduction of 2 Ca are also shown to be low here. This is most likely an artifact caused by less Fura-2 availability, thereby limiting the amount of cytoplasmic Ca^{2+} that can be measured.

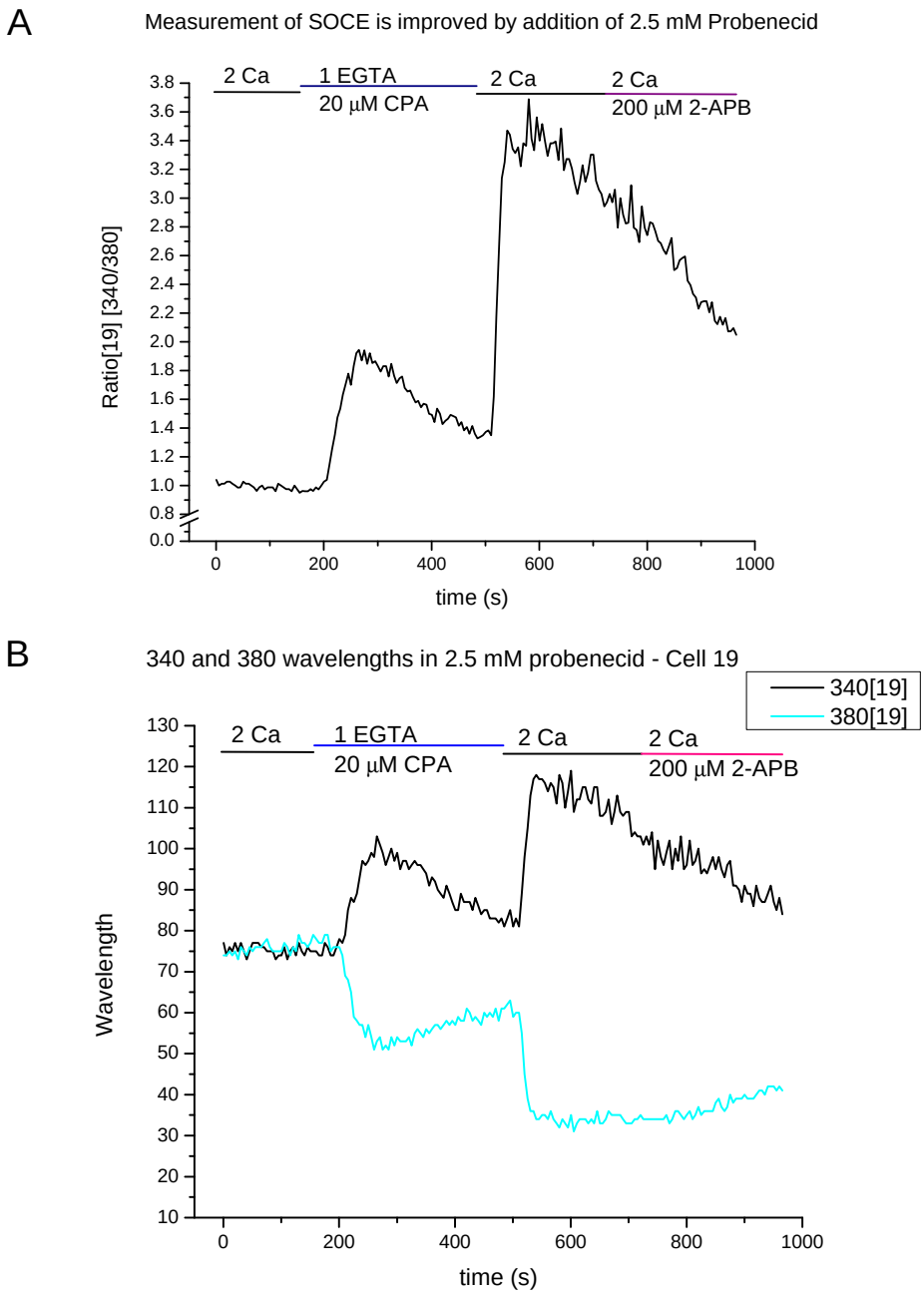

Figure 3.6: The presence of 2.5 mM probenecid improves dye loading in S2 cells. (**A**) The ratio of the 340 nm and 380 nm wavelengths of an individual cell during the course of a perfusion experiment where 2.5 mM probenecid was included in the incubation solution. (**B**) The individual 340 nm and 380 nm wavelength values, which produced the ratio seen in **A**.

Figure 3.6A shows a sample recording from a cell incubated with DLS containing 2.5 mM probenecid. The ratio is robust and provides better resolution than the trace in figure 3.5. Figure 3.6B gives the individual 340 nm and 380 nm wavelengths which were used to obtain the ratio in A. We are able to clearly see the reciprocal nature of the 340 nm and 380 nm wavelength values. The steady decline of the values over the course of the experiment is no longer apparent. Probenecid has stopped or greatly slowed leakage of Fura-2 from the cytosol. As a result, we are able to record higher Ca^{2+} transients as more Fura-2 is available as the experiment proceeds, compared to cells loaded without probenecid. This is readily apparent in the SOCE portion of the trace.

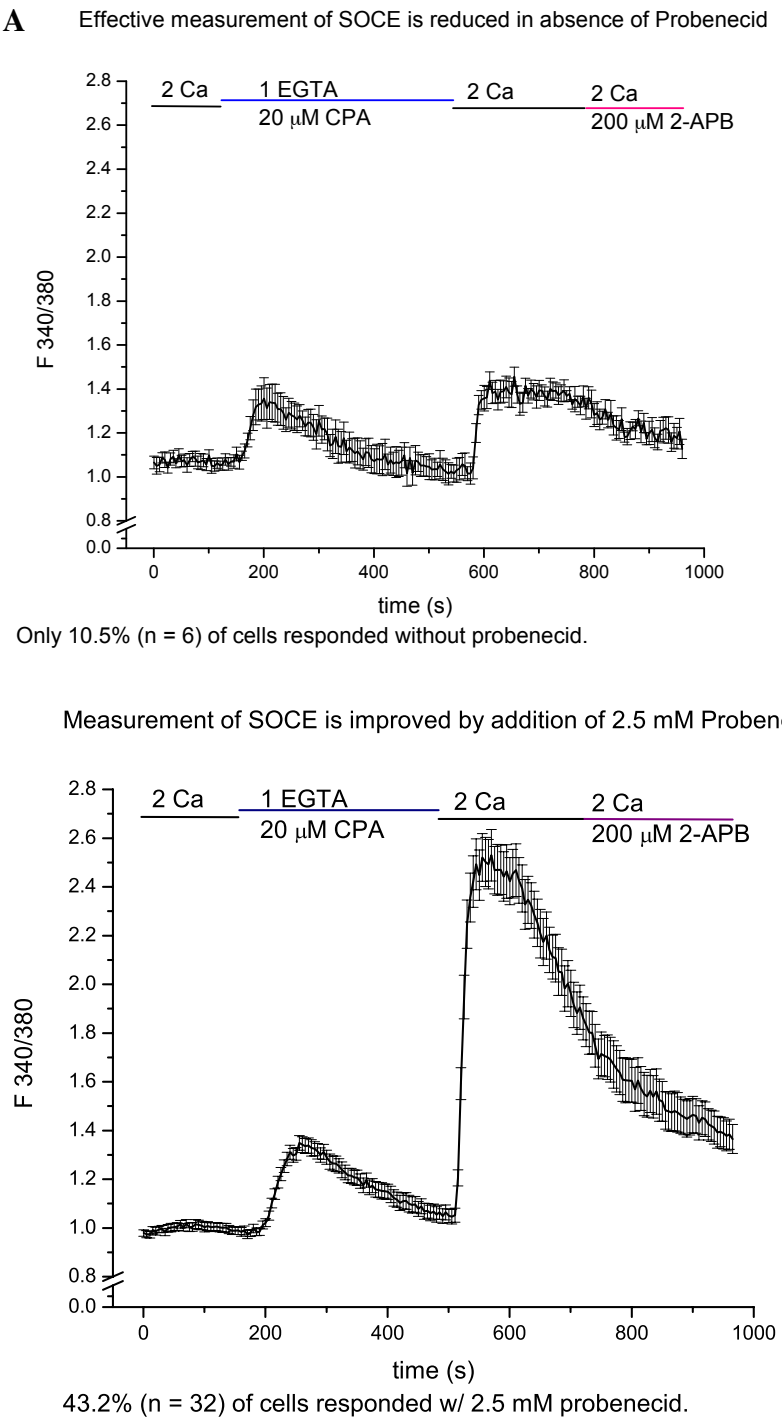

Figure 3.7: Addition of Probenecid improves Ca^{2+} recordings. (**A**) Recordings taken from a population of cells incubated in dye-loading solution that did not contain probenecid (**B**) Recordings taken from a population of cells incubated in dye-loading solution that contained 2.5 mM probenecid.

Figure 3.7 shows a population of cells loaded without (A) and with (B) probenecid. We are able to observe a larger Ca^{2+} transient, due to more Fura-2 being available. Also, addition of probenecid results in more cells meeting the selection criteria for data collection. This can be attributed to Fura-2 retention in probenecid-treated S2 cells. The result is more dye being available at the start of the experiment, and as it progresses.

Unhealthy cells, cells with damaged plasma membranes may also be omitted from the data set in a reliable, unbiased manner after probenecid treatment. Such cells would still display characteristics of untreated cells such as pronounced, persistent dye leakage.

Conditions for selecting data were formulated after examining individual 340 nm and 380 nm wavelength traces for probenecid-treated and untreated cells. Three out of six cells in A, had either 340 nm or 380 nm wavelength values below 40. This led us to use 40 as a cutoff value for data selection. For the S2 cells selected, both the 340 nm and 380 nm wavelength values stayed at or above 40 during the initial 2 Ca perfusion. This allowed for elimination of cells which were poorly loaded with Fura dye.

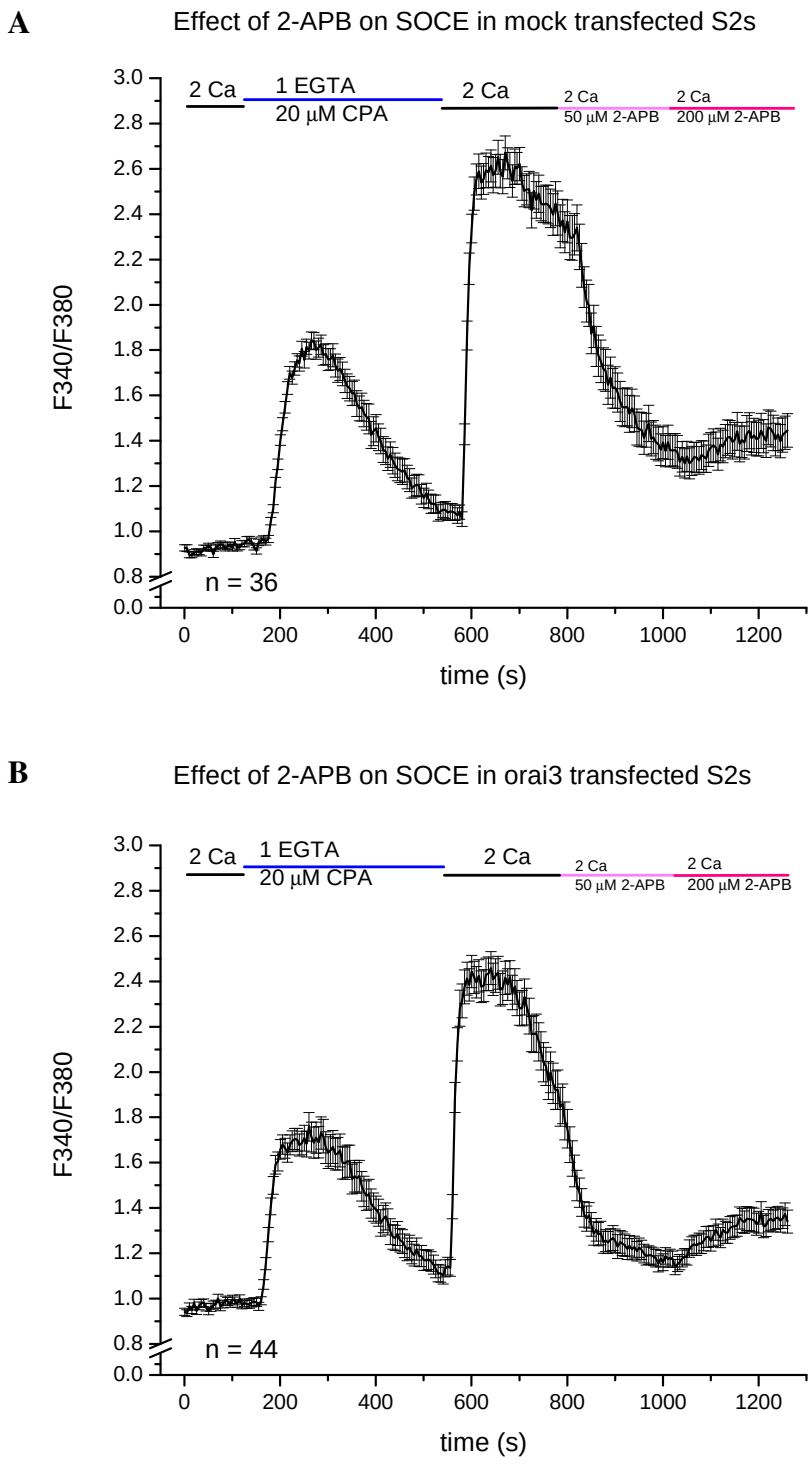

Figure 3.8: Ca^{2+} measurements in transfected S2 cells perfused with 2-APB. The lines above the trace are labeled with the solutions perfused during those times. **A**) A trace of mock-transfected S2s showing the effect of 2-APB on SOCE. **B**) A trace of Orai3-transfected S2s showing the effect of 2-APB on SOCE.

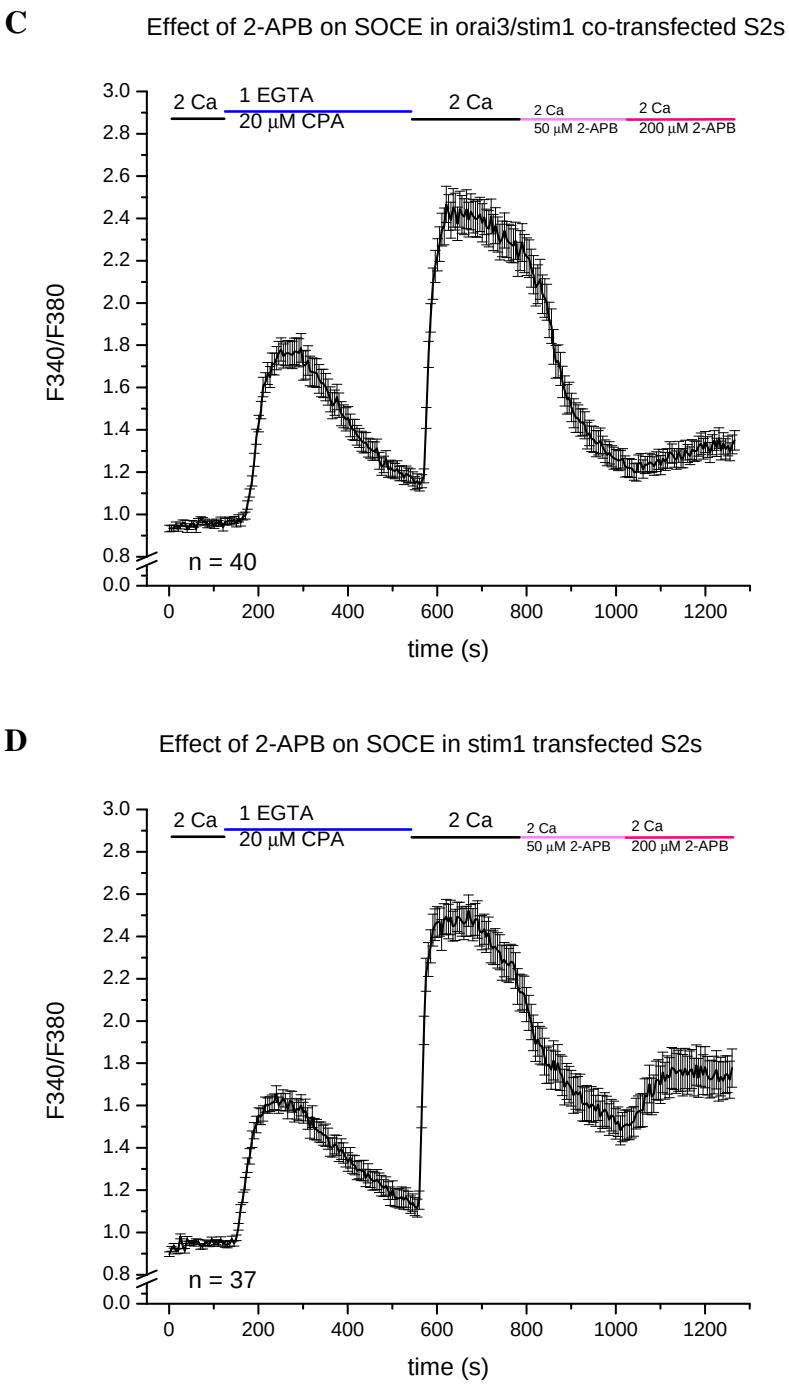

Figure 3.8: Ca^{2+} measurements in transfected S2 cells perfused with 2-APB. The lines above the trace are labeled with the solutions perfused during those times. **C**) Sample trace of Orai3+STIM1-transfected S2s showing the effect of 2-APB on SOCE. **D**) Sample trace of STIM1-transfected S2s showing the effect of 2-APB on SOCE.

The composite in Figure 3.8 shows representative traces for Ca^{2+} imaging experiments where S2 cells have been mock-transfected or transfected with Orai3, STIM1, or Orai3+STIM1. In Figure 3.8A we see an average of several traces giving the result of an experiment done on mock-transfected S2s. Initially, the 2 Ca response of these mock-transfected S2s is relatively stable. Upon introduction of 20 μM CPA in 1 EGTA, we observe an increase in the F340/F380 ratio. This indicates an increase in cytosolic free Ca^{2+}, resulting from leakage of Ca^{2+} from the ER. This Ca^{2+} leak achieves a maximum and subsequently declines. The decline phase is indicative of Ca^{2+} being pumped out of the cell, shuttled to non-ER compartments, such as the mitochondria, or being bound by cytosolic Ca^{2+} chelators. Transport of Ca^{2+} to the ER is prevented by CPA, which blocks the SERCA pump.

After $\sim$7 minutes of perfusion in 1 EGTA/20 μM CPA, Ca^{2+} is reintroduced. The mock-transfected S2s then exhibit SOCE, and a second Ca^{2+} transient forms at this stage. The maximal Ca^{2+} entry after 2 Ca reintroduction is greater than maximal Ca^{2+} release from the ER. *dOrai* channels responsible for SOCE in S2 cells are able to open quickly, allowing Ca^{2+} into the cell shortly after switching to the 2 Ca solution. We eventually begin to see less Ca^{2+}, which can be attributed to *dOrai* channels closing, slowing Ca^{2+} entry.

After 4 minutes in 2 Ca, 50 μM 2-APB is added to the perfusion solution. We see for the mock-transfected S2 cells, that the gradual decline in Ca^{2+} becomes sharper, shortly after addition of 2-APB. This is expected because at these concentrations 2-APB is inhibitory for *dOrai* (48). The decline in Ca^{2+} continues during the 4 minutes in 50 μM 2-APB.

After 4 minutes in 2 Ca with 50 μM 2-APB, the 2-APB concentration is increased to 200 μM 2-APB. This solution was perfused across the cells for another 4 minutes and then the experiment was stopped. During this time we observe what seems to be a slight increase. The overlap of the error bars along the trace indicate that, while there is a trend toward an increase, further analysis is required to determine its significance. In order to address the question of what happens to Ca^{2+}, the area under the curve was calculated for

each 4-minute section after store-depletion occurred for each group of transfected cells.

Figure 3.8B shows an average trace of an experiment performed on Orai3-transfected S2 cells. The initial and store-depletion phases are similar to those in the mock-transfected S2s. 2 Ca reintroduction shows a swift onset of SOCE. The expected increase in Ca^{2+} after addition of 50 μM 2-APB was not seen, however. Addition of 200 μM 2-APB seemed to result in a marginal increase in Ca^{2+} entry. The Ca^{2+} content of this 200 μM 2-APB phase was analyzed further and no significant change from the mock was found (see Figure 3.9).

Since no distinct effect of 2-APB was observed in S2s transfected with Orai3 only, Orai3+STIM1 transfections were performed. We reasoned that human Orai3 may require a human STIM1 protein for coupling, rather than the background *dStim* natively expressed in S2 cells. A trace for one of these experiments is provided in Figure 3.8C. The store-depletion and SOCE phases again seem similar to that of the mock- and Orai3-transfected cells. When treated with 50 and 200 μM 2-APB, no clear trend was visible compared to the mock- or Orai3-transfected cells.

In Figure 3.8D a similar experiment was performed, but on STIM1-transfected S2s. Here, the store-depletion and SOCE phases after 2 Ca reintroduction are similar to mock and other transfections. Interestingly, addition of 50 μM 2-APB in the STIM1 only transfected cells, was less effective at slowing Ca^{2+} entry than in the other transfections. When 200 μM 2-APB was added, a clear increase in cytosolic Ca^{2+} was observed.

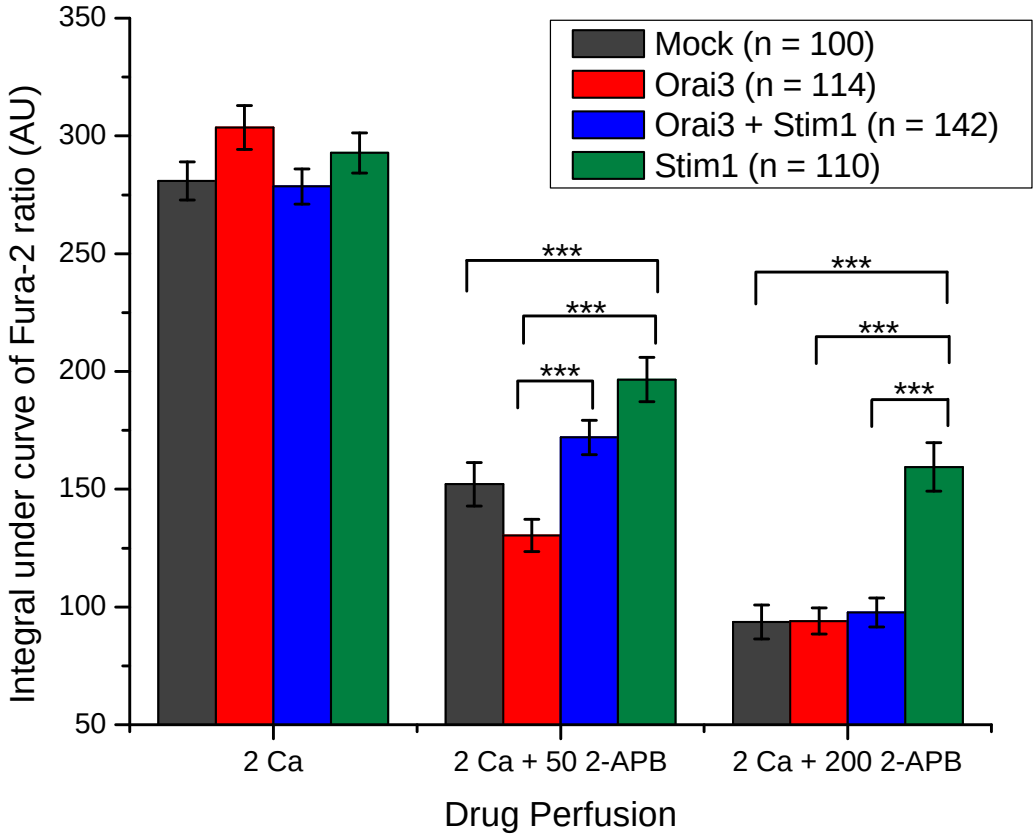

Figure 3.9: Cytoplasmic Ca^{2+} content in transfected S2 cells. The bars represent area under the curve analysis for segments where **2 Ca**, **2 Ca + 50 μM 2-APB**, or **2 Ca + 200 μM 2-APB** were used to perfuse transfected S2 cells. The transfection groups are indicated in the legend. Significant differences between the transfected groups at the 0.05 significance level are indicated by ***. No significant difference was found between the 2 Ca perfusion group. Significant differences were found between the 2 Ca + 50 μM 2-APB and 2 Ca + 200 μM 2-APB perfusion groups.

Figure 3.9 displays the results of area under the curve (AUC) analysis on the three phases of treatment after store-depletion. By doing AUC analysis, the ratios generated by Fura-2 recordings were translated into cytosolic Ca^{2+} content of arbitrary units. The three groups in the bar graph correspond to perfusion with 2 Ca, 2 Ca + 50 μM 2-APB, and 2 Ca + 200 μM 2-APB. The perfusion time for each group was 4 minutes. A one way ANOVA was used to determine if there were significant differences in the experimental groups. If significant differences were found, Tukey's studentized range test, was used to determine

where significant differences lie between the transfection groups.

The 2 Ca group represents an untreated period of SOCE in the transfection groups. Statistical analysis showed no significant change in cytosolic Ca^{2+} for this group. Functional Orai3 Ca^{2+} channels were expected to increase the levels of cytosolic Ca^{2+} during SOCE. That this was not observed may be due to the inability of Orai3 to express *in the membrane*, a possibility addressed in the discussion.

The 2 Ca + 50 2-APB experiments did show significant differences in this treatment group. Significant differences existed between Orai3+STIM1-transfected cells and the Orai3 only transfected group. There were also significant differences between STIM1 only transfected cells and Orai3 only transfected cells. For both of the groups described above, the Orai3 only group showed much less cytosolic Ca^{2+}, which was unexpected. A significant difference was also found between mock-transfected and STIM1-transfected cells, with the STIM1-transfected group having higher levels of cytosolic calcium than the mock-transfected group. The significant differences for all of the above was $p < 0.0001$ at the 0.05 significance level.

The 2 Ca + 200 2-APB showed a small but significant difference only between the STIM1-transfected cells and all the other groups. Again, an unexpected result which is discussed further below.

Discussion

As demonstrated in figures 3.1 and 3.2 the ligation of the inserts and subsequent cloning of pucHygMT-Orai3 and pucHygMT-STIM1 were successful. *Drosophila* vectors *capable* of expressing mammalian Orai3 and STIM1 genes in S2 cells were created, satisfying specific aim #1.

Figures 3.3 and 3.4 then showed induction of Orai3 and STIM1 *gene expression* from these vectors. This demonstrated that both vector constructs actually expressed these mammalian genes in *Drosophila* S2 cells, satisfying specific aim #2. Having carried out the objectives in specific aims #1 and #2, we moved on to address specific aim #3: assessing the effect of 2-APB on Orai3 channels. As mentioned previously, concentrations of ≥ 50 μM 2-APB will activate mammalian Orai3 channels.

Initial attempts at taking Ca^{2+} measurements in S2 cells were thwarted by leakage of Fura-2, the Ca^{2+} dye being used, from these cells. As demonstrated in figures 3.5, 3.6 and 3.7 addition of the anion transport inhibitor probenecid was crucial to recording satisfactory calcium transients. We see that omission of probenecid led to ratio measurements of SOCE transients which were lower than those recorded when probenecid was present. Leakage of Fura-2, would have resulted in a gradual elevation of the significance of the background fluorescence. The lower ratio maxima for SOCE transients then is likely due to the low ratio caused by background fluorescence in the the cells not treated with probenecid. We see that addition of probenecid reduced dye leakage by blocking the transporters responsible, and resulted in better measurements of S2 cell populations. This demonstrates that the use of

probenecid for Ca^{2+} recordings of *Drosophila* S2 cells is necessary for obtaining quality data (47).

After solving the issue of recording Ca^{2+} transients, assessing the effect of 2-APB on S2 cells expressing Orai3 was possible. Our hypothesis, that gene expression of mammalian Orai3 in *Drosophila* S2s would result in Ca^{2+} channels that behaved similarly to those in mammalian cells expressing Orai3 proved incorrect. As seen by the results presented in figures 3.8 and 3.9, Orai3 channel behavior in our *Drosophila* expression system was anomalous, no increase in SOCE due to Orai3 was observed (2 Ca column, figure 3.9). Aims #1 and 2 were achieved, but testing of aim #3 showed that the expression model requires further optimization.

An unexpected and interesting result from this study was the ability of STIM1 to cause an increase in cytosolic Ca^{2+}. The results in figure 3.8 for the STIM1 only transfection hint at less *deactivation* of *dOrai* occurring in 50 μM 2-APB compared to the mock transfection. Addition of 200 μM 2-APB to STIM1 only transfected S2s resulted in a clear increase in cytosolic calcium indicative of channel opening. One explanation is that another Ca^{2+} channel opened due to the combination of STIM1 and 2-APB. It may also be that 200 μM 2-APB is interacting with STIM1 leading to non-specific effects on *dOrai*. As this is only present in the STIM1 transfected cells, and since the amount of STIM1 DNA used in STIM1 and Orai3+STIM1 transfections was the same (2 μg) this suggests an effector+2-APB interaction in the absence of Orai3.

There are several possibilities for why Orai3, either alone or with STIM1, did not display the expected Ca^{2+} increase after addition of 50 or 200 μM 2-APB. The most obvious is that while Orai3 RNA production was induced with $CuSO_4$, actual protein production did not occur by the time of the experiments. Another possibility is that the transfection efficiency was consistently low with the transfection reagent and pucHygMT-Orai3 DNA. This may have resulted in poor expression of Orai3 and a paucity of Orai3 protein translation, leading to a deficiency in Orai3 channels expressed at the cellular surface. Another

possibility is that, because of how closely related Orai3 and *dOrai* are – a BLAST comparison shows a 64% nucleotide sequence similarity – Orai3 forms heteromers with *dOrai*, and adopts a phenotype primarily *dOrai* dominated in nature.

Given that STIM1 expression results in an unexpected phenotype, it is unlikely that Orai3, the smaller protein which was made in a similar manner, does not express. It is more likely that interactions with the closely related *dOrai* result in heteromeric channels, and it is the output from those channels that we are investigating.

Transfection of Orai3 with STIM1 did lead to a significant increase in cytosolic Ca^{2+} compared to Orai3 only transfected cells (see figure 3.9). This suggests that *dStim* is not sufficient for Orai3 function.

Future work on this project will involve testing the possibilities presented above, for why Orai3 activation did not occur after 2-APB treatment. The generation of stable cell lines using the hygromycin B resistance conferred by pucHygroMT is underway. While creating clonal populations of stably selected S2 cells is possible, reports indicate that the additional effort does not seem worthwhile (37). Expression levels for high-expressing clones seem similar to those from a polyclonal population (37). Stable lines expressing Orai3 and STIM1 together will facilitate experiments needed to test these possibilities.

Protein expression of Orai3 can be tested by isolating proteins from transfected cells and performing Western Blot analysis using antibodies to Orai3. Testing for interference from native *dOrai* by performing RNA_i knockdown will address the issue of *dOrai* influencing the Orai3 channel phenotypes. Beyond the potential issue of *dOrai* affecting Orai3 function and/or expression, RNA_i knockdown of *dOrai* allows study of Orai3 channels in isolation on a *dOrai*-free background. This will be useful for defining Orai3 channel function, as opposed to general SOCE, to which Orai3 may contribute.

4.1 Conclusion

The creation of an expression system for mammalian Orai Ca^{2+} channels to be used for drug discovery purposes was begun in this study. The proteins selected to probe the feasibility of using such a system were the mammalian Orai3 Ca^{2+} channel, and mammalian Ca^{2+} sensor STIM1. Constructs for expression in S2 cells were created and were able to successfully express genes from both Orai3, and STIM1. Our *Drosophila* system was not able to reproduce the function of the Orai3 channel in the presence of the known effector 2-APB, highlighting the need for further refinement, before use in future drug studies. Provided that the issues with channel expression are solved, the system has the potential to be a very useful tool, for study of not just Orai3, but the entire Orai family.

The system is effective in inducing RNA expression of Orai3 and STIM1, however, and is currently being used to generate stable cell lines to further this study. Given the importance of SOCE to the adaptive immune response and related disease states, this initial work and future studies based upon it, have the potential to be important vehicles for contributing to the body of knowledge in the field of Ca^{2+} metabolism. Studies of diseases resulting from disrupted Ca^{2+} homeostasis, including forms of cancer and autoimmune diseases, may also benefit from the creation of this expression system.

Bibliography

1. ASMILD, M. AND WILLUMSEN, N. J. 2000. Chloride channels in the plasma membrane of a foetal Drosophila cell line, S2. *Pflügers Archiv : European journal of physiology 439,* 6, 759–64.

2. BAKSH, S. AND BURAKOFF, S. J. 2000. The role of calcineurin in lymphocyte activation. *Seminars in immunology 12,* 4, 405–15.

3. BAUM, B. AND CHERBAS, L. 2008. Drosophila cell lines as model systems and as an experimental tool. In *Drosophila: Methods and Protocols*, C. Dahmann, Ed. Vol. 420. Humana Press, Totowa, NJ, Chapter 25, 391–424.

4. BERRIDGE, M. J., BOOTMAN, M. D., AND RODERICK, H. L. 2003. Calcium signalling: dynamics, homeostasis and remodelling. *Nature Reviews Molecular Cell Biology 4,* 7, 517–529.

5. BERRIDGE, M. J., LIPP, P., AND BOOTMAN, M. D. 2000. The versatility and universality of calcium signalling. *Nature Reviews Molecular Cell Biology 1,* 1, 11–21.

6. BILMEN, J. G., WOOTTON, L. L., GODFREY, R. E., SMART, O. S., AND MICHELANGELI, F. 2002. Inhibition of SERCA Ca2+ pumps by 2-aminoethoxydiphenyl borate (2-APB). *European Journal of Biochemistry 269,* 15, 3678–3687.

7. BUNCH, T., GRINBLAT, Y., AND GOLDSTEIN, L. 1988. Characterization and use of the Drosophila metallothionein promoter in cultured Drosophila melanogaster cells. *Nucleic acids research 16,* 3, 1043–61.

8. CHUMAKOV, K. 1994. Reverse transcriptase can inhibit PCR and stimulate primer-dimer formation. *PCR Methods and Applications 4,* 1, 62–64.

9. CORDOVA, D., DELPECH, V. R., SATTELLE, D. B., AND RAUH, J. J. 2003. Spatiotemporal calcium signaling in a Drosophila melanogaster cell line stably expressing a Drosophila muscarinic acetylcholine receptor. *Invertebrate neuroscience 5,* 1, 19–28.

10. DELLIS, O., MERCIER, P., AND CHOMIENNE, C. 2011. The boron-oxygen core of borinate esters is responsible for the store-operated calcium entry potentiation ability. *BMC pharmacology 11,* 1, 1.

11. DI VIRGILIO, F., STEINBERG, T. H., AND SILVERSTEIN, S. C. 1990. Inhibition of Fura-2 sequestration and secretion with organic anion transport blockers. *Cell calcium 11,* 2-3, 57–62.

12. EBLE, J. A., WUCHERPFENNIG, K. W., GAUTHIER, L., DERSCH, P., KRUKONIS, E., ISBERG, R. R., AND HEMLER, M. E. 1998. Recombinant soluble human alpha 3 beta 1 integrin: purification, processing, regulation, and specific binding to laminin-5 and invasin in a mutually exclusive manner. *Biochemistry 37,* 31, 10945–55.

13. EID, J.-P., ARIAS, A. M., ROBERTSON, H., HIME, G. R., AND DZIADEK, M. 2008. The Drosophila STIM1 orthologue, dSTIM, has roles in cell fate specification and tissue patterning. *BMC developmental biology 8,* 1, 104.

14. FESKE, S., GWACK, Y., PRAKRIYA, M., SRIKANTH, S., PUPPEL, S.-H., TANASA, B., HOGAN, P. G., LEWIS, R. S., DALY, M., AND RAO, A. 2006. A mutation in Orai1 causes immune deficiency by abrogating CRAC channel function. *Nature 441,* 7090, 179–185.

15. GOTO, J.-I., SUZUKI, A. Z., OZAKI, S., MATSUMOTO, N., NAKAMURA, T., EBISUI, E., FLEIG, A., PENNER, R., AND MIKOSHIBA, K. 2010. Two novel 2-aminoethyl diphenylborinate (2-APB) analogues differentially activate and inhibit store-operated Ca(2+) entry via STIM proteins. *Cell calcium 47,* 1, 1–10.

16. GWACK, Y., SRIKANTH, S., FESKE, S., CRUZ-GUILLOTY, F., OH-HORA, M., NEEMS, D., HOGAN, P., AND RAO, A. 2007. Biochemical and functional characterization of Orai proteins. *Journal of Biological Chemistry 282,* 22, 16232–43.

17. HOTH, M. AND PENNER, R. 1992. Depletion of intracellular calcium stores activates a calcium current in mast cells. *Nature 355,* 6358, 353–356.

18. JOHANSON, K., APPELBAUM, E., DOYLE, M., HENSLEY, P., ZHAO, B., ABDEL-MEGUID, S., YOUNG, P., COOK, R., CARR, S., MATICO, R., AND OTHERS. 1995. Binding Interactions of Human Interleukin 5 with Its Receptor α Subunit. *Journal of Biological Chemistry 270,* 16, 9459–9471.

19. LAMBERT, D. G. 2006. *Calcium signaling protocols*, 2nd ed. Methods in molecular biology. Humana Press, Totowa, NJ.

20. LANSDELL, S. J., COLLINS, T., YABE, A., GEE, V. J., GIBB, A. J., AND MILLAR, N. S. 2008. Host-cell specific effects of the nicotinic acetylcholine receptor chaperone RIC-3 revealed by a comparison of human and Drosophila RIC-3 homologues. *Journal of neurochemistry 105,* 5, 1573–81.

21. LEWIS, R. S. 2001. Calcium signaling mechanisms in T lymphocytes. *Annual review of immunology 19*, 497–521.

22. LIOU, J., KIM, M. L., HEO, W. D., JONES, J. T., MYERS, J. W., FERRELL, J. E., AND MEYER, T. 2005. STIM is a Ca2+ sensor essential for Ca2+-store-depletion-triggered Ca2+ influx. *Current Biology 15,* 13, 1235–1241.

23. LIOUDYNO, M. I., KOZAK, J. A., PENNA, A., SAFRINA, O., ZHANG, S. L., SEN, D., ROOS, J., STAUDERMAN, K. A., AND CAHALAN, M. D. 2008. Orai1 and STIM1 move to the immunological synapse and are up-regulated during T cell activation. *Proceedings of the National Academy of Sciences of the United States of America 105,* 6, 2011–16.

24. LUCE-FEDROW, A., VON OHLEN, T., BOYLE, D., GANTA, R. R., AND CHAPES, S. K. 2008. Use of Drosophila S2 cells as a model for studying Ehrlichia chaffeensis infections. *Applied and environmental microbiology 74,* 6, 1886–91.

25. MASEREEUW, R., VAN PELT, A., VAN OS, S., WILLEMS, P., SMITS, P., AND RUSSEL, F. 2000. Probenecid interferes with renal oxidative metabolism: A potential pitfall in its use as an inhibitor of drug transport. *British journal of pharmacology 131,* 1, 57–62.

26. MIGNEN, O., THOMPSON, J. L., AND SHUTTLEWORTH, T. J. 2008. Both Orai1 and Orai3 are essential components of the arachidonate-regulated Ca2+-selective (ARC) channels. *The Journal of physiology 586,* 1, 185–95.

27. MILLAR, N. S., BAYLIS, H. A., REAPER, C., BUNTING, R., MASON, W. T., AND SATTELLE, D. B. 1995. Functional expression of a cloned Drosophila muscarinic acetylcholine receptor in a stable Drosophila cell line. *The Journal of experimental biology 198,* Pt 9, 1843–50.

28. MONCOQ, K., TRIEBER, C. A., AND YOUNG, H. S. 2007. The molecular basis for cyclopiazonic acid inhibition of the sarcoplasmic reticulum calcium pump. *The Journal of biological chemistry 282,* 13, 9748–57.

29. MOTIANI, R. K., ABDULLAEV, I. F., AND TREBAK, M. 2010. A novel native store-operated calcium channel encoded by Orai3: selective requirement of Orai3 versus Orai1 in estrogen receptor-positive versus estrogen receptor-negative breast cancer cells. *The Journal of biological chemistry 285,* 25, 19173–83.

30. PFEIFER, T. 1998. Expression of heterologous proteins in stable insect cell culture. *Current opinion in biotechnology 9,* 5, 518–21.

31. PRAKRIYA, M., FESKE, S., GWACK, Y., SRIKANTH, S., RAO, A., AND HOGAN, P. G. 2006. Orai1 is an essential pore subunit of the CRAC channel. *Nature 443,* 7108, 230–233.

32. PRAKRIYA, M. AND LEWIS, R. S. 2001. Potentiation and inhibition of Ca(2+) release-activated Ca(2+) channels by 2-aminoethyldiphenyl borate (2-APB) occurs independently of IP(3) receptors. *The Journal of physiology 536,* 1, 3–19.

33. PUTNEY, J. W. 1986. A model for receptor-regulated calcium entry. *Cell Calcium 7,* 1, 1–12.

34. PUTNEY, J. W. 2006. *Calcium signaling*, 2nd ed. Methods in signal transduction. CRC Press, Boca Raton, FL.

35. ROOS, J., DIGREGORIO, P. J., YEROMIN, A. V., OHLSEN, K., LIOUDYNO, M., ZHANG, S., SAFRINA, O., KOZAK, J. A., WAGNER, S. L., CAHALAN, M. D., VELIÇELEBI, G., AND STAUDERMAN, K. A. 2005. STIM1, an essential and conserved component of store-operated Ca2+ channel function. *The Journal of cell biology 169,* 3, 435–45.

36. SAMBROOK, J. AND RUSSELL, D. W. 2001. *Molecular cloning: a laboratory manual*, 3rd ed. Cold Spring Harbor Laboratory Press, Cold Spring Harbor, NY.

37. SCHETZ, J. A. AND SHANKAR, E. P. N. 2004. Protein expression in the Drosophila Schneider 2 cell system. *Current protocols in neuroscience Chapter 4*, 4.16.1–15.

38. SCHNEIDER, I. 1972. Cell lines derived from late embryonic stages of Drosophila melanogaster. *Journal of embryology and experimental morphology 27,* 2, 353–65.

39. SMYTH, J., HWANG, S., TOMITA, T., DEHAVEN, W., MERCER, J., AND PUTNEY, J. 2010. Activation and regulation of store-operated calcium entry. *Journal of Cellular and Molecular Medicine 14,* 10, 2337–2349.

40. SOBOLOFF, J., SPASSOVA, M. A., HEWAVITHARANA, T., HE, L.-P., XU, W., JOHNSTONE, L. S., DZIADEK, M. A., AND GILL, D. L. 2006. STIM2 is an inhibitor of STIM1-mediated store-operated Ca2+ Entry. *Current Biology 16,* 14, 1465–1470.

41. STREB, H., IRVINE, R. F., BERRIDGE, M. J., AND SCHULZ, I. 1983. Release of Ca2+ from a nonmitochondrial intracellular store in pancreatic acinar cells by inositol-1,4,5-trisphosphate. *Nature 306,* 5938, 67–69.

42. TAYLOR, C. 2006. Store-operated Ca2+ entry: a STIMulating stOrai. *Trends in biochemical sciences 31,* 11, 597–601.

43. TIMMERMAN, L. A., CLIPSTONE, N. A., HO, S. N., NORTHROP, J. P., AND CRABTREE, G. R. 1996. Rapid shuttling of NF-AT in discrimination of Ca2+ signals and immunosuppression. *Nature 383,* 6603, 837–840.

44. VIG, M., PEINELT, C., BECK, A., KOOMOA, D. L., RABAH, D., KOBLAN-HUBERSON, M., KRAFT, S., TURNER, H., FLEIG, A., PENNER, R., AND KINET, J.-P. 2006. CRACM1 is a plasma membrane protein essential for store-operated Ca2+ entry. *Science 312,* 5777, 1220–23.

45. WILLIAMS, R., MANJI, S., PARKER, N., HANCOCK, M., VAN STEKELENBURG, L., EID, J., SENIOR, P., KAZENWADEL, J., SHANDALA, T., SAINT, R., SMITH, P. J., AND DZIADEK, M. A. 2001. Identification and characterization of the STIM (stromal interaction molecule) gene family: coding for a novel class of transmembrane proteins. *Biochemical Journal 357,* 3, 673–685.

46. XU, Y.-B., LI, H.-P., ZHANG, J.-B., SONG, B., CHEN, F.-F., DUAN, X.-J., XU, H.-Q., AND LIAO, Y.-C. 2010. Disruption of the chitin synthase gene CHS1 from Fusarium

asiaticum results in an altered structure of cell walls and reduced virulence. *Fungal genetics and biology 47,* 3, 205–15.

47. YAGODIN, S., PIVOVAROVA, N. B., ANDREWS, S. B., AND SATTELLE, D. B. 1999. Functional characterization of thapsigargin and agonist-insensitive acidic Ca2+ stores in Drosophila melanogaster S2 cell lines. *Cell calcium 25,* 6, 429–38.

48. YEROMIN, A. V., ROOS, J., A STAUDERMAN, K., AND CAHALAN, M. D. 2004. A store-operated calcium channel in Drosophila S2 cells. *The Journal of general physiology 123,* 2, 167–182.

49. ZHANG, S. L., KOZAK, J. A., JIANG, W., YEROMIN, A. V., CHEN, J., YU, Y., PENNA, A., SHEN, W., CHI, V., AND CAHALAN, M. D. 2008. Store-dependent and -independent modes regulating Ca2+ release-activated Ca2+ channel activity of human Orai1 and Orai3. *The Journal of biological chemistry 283,* 25, 17662–71.

50. ZHANG, S. L., YEROMIN, A. V., ZHANG, X. H.-F., YU, Y., SAFRINA, O., PENNA, A., ROOS, J., STAUDERMAN, K. A., AND CAHALAN, M. D. 2006. Genome-wide RNAi screen of Ca(2+) influx identifies genes that regulate Ca(2+) release-activated Ca(2+) channel activity. *Proceedings of the National Academy of Sciences of the United States of America 103,* 24, 9357–62.

51. ZHANG, S. L., YU, Y., ROOS, J., KOZAK, J. A., DEERINCK, T. J., ELLISMAN, M. H., STAUDERMAN, K. A., AND CAHALAN, M. D. 2005. STIM1 is a Ca2+ sensor that activates CRAC channels and migrates from the Ca2+ store to the plasma membrane. *Nature 437,* 7060, 902–905.

52. ZWEIFACH, A. AND LEWIS, R. S. 1993. Mitogen-regulated Ca2+ current of T lymphocytes is activated by depletion of intracellular Ca2+ stores. *Proceedings of the National Academy of Sciences of the United States of America 90,* 13, 6295–99.